Plasma Sources Science and Technology

TOPICAL REVIEW

Streamer breakdown: cathode spot formation, Trichel pulses and cathode-sheath instabilities

To cite this article: Mirko ernák *et al* 2020 *Plasma Sources Sci. Technol.* **29** 013001

IOP Publishing Plasma Sources Science and Technology
Plasma Sources Sci. Technol. **29** (2020) 013001 (31pp) https://doi.org/10.1088/1361-6595/ab5051

Topical Review

Streamer breakdown: cathode spot formation, Trichel pulses and cathode-sheath instabilities

Mirko Černák, Tomáš Hoder and Zdeněk Bonaventura

Department of Physical Electronics, Masaryk University, Kotlářská 2, 61137 Brno, Czech Republic

E-mail: cernak@physics.muni.cz

Received 20 October 2017, revised 8 August 2019
Accepted for publication 22 October 2019
Published 20 December 2019

Abstract

The review provides an up-to-date overview and discussion of phenomena related to positive streamer breakdowns in short uniform and non-uniform field (corona) gaps. The terminology used to specify different types of streamer phenomena is critically discussed in light of a unified theory of high-pressure gas discharges describing the sequence of ionization events from initial electron avalanches up to a partial or complete breakdown. The emphasis is given to the understanding of the formation of an active cathode spot by the streamer arrival to the cathode, which is the critical but still obscure phase of the breakdown development. Based on the analysis including a computer simulation model a hypothesis is advanced that also such widely studied and practically important gas discharge phenomena as negative corona Trichel pulses and fast ionization instabilities in cathode regions of high-pressure gas discharges are due to the formation of positive streamers in the immediate cathode vicinity. The proposed hypothesis offers attractive feature of the unification of a wide scale of high-pressure gas discharges within the general class of positive streamer initiated breakdown phenomena. Moreover, it provides indications for further study in the field both by experiment and computer simulations.

Keywords: electron avalanche, Trichel pulse, streamer–cathode interaction, cathode spot, cathode-sheath instability, breakdown, streamer and spark

1. Introduction

Already in 1857 Siemens [1] discovered that the filamentary dielectric barrier discharge (DBDs) can be effectively used to generate 'ozonizing air'. In 1928 Rogowski [2] observed that the pulsed voltage breakdown in wide ambient air gaps is two orders faster than can be expected on the base of the gas ionization by successive electron avalanches linked by secondary electron emission from the cathode. Now, the gas ionization phenomena related to these pioneering discoveries in the field of gas discharge physics are well interpreted and understood in terms of the concept of 'streamers' first proposed by Raether [3], and by Loeb and Meek [4] in 1930s. The streamer concept has proven very useful for fundamental understanding of a multitude of gas discharge phenomena [5] and has pushed the physics backing new applications of high-pressure gas discharges [6–8].

Nevetheless, in view of the maturity and proven usefulness of the streamer concept, the scientific and engineering literature on the subject is still surprisingly inconsistent, which results in the persistent and even increasing gap between the basic research and applications. For example, the engineering community in the field of applied gas discharge physics is using the streamer concept often only in its obsolete 'single-avalanche' form [9, 10], or the term 'streamer' is omitted even by respected authors in the field of atmospheric-pressure plasma sources [11] and high voltage systems in air [12]. In our opinion the problem is caused mainly by the lack of a consistent and generally accepted streamer theory [13].

In our topical review, an attempt is being made to clarify the streamer terminology and to identify weakest links in the understanding of ionization phenomena leading to the high-pressure gas breakdown starting from initiatory electrons, via a streamer discharge phase, to the final arc or spark.

Nowadays, the numerical simulations are crucial to our understanding of complex streamer and breakdown phenomena [6]. Therefore, the success of computer simulation models in explaining the sequence of events leading to the streamer breakdown can be regarded as a measure of the theoretical understanding the phenomena leading to the breakdown. Based on this, it appears that the positive streamer arrival to the cathode, which is very difficult to study both by experiment and computer simulations, is the most obscure, but very critical link in the chain of sequences leading to streamer breakdown.

Therefore, in the review we will provide up-to-date overview of phenomena related to the positive streamer arrival to the cathode and attempt to clarify their role in high-pressure gas breakdowns. Also, contrary to commonly held belief, we will advance hypothesis that such widely studied and practically important gas discharge phenomena as negative corona Trichel pulses (TPs) and instabilities in cathode regions of high-pressure gas discharges resulting in arcing are also due to a positive streamer generated in the immediate cathode vicinity and its arrival to the cathode.

The paper is structured as follows. Section 2 presents the historical progression and development of the relevant experimental techniques and terminology. Section 3 reviews the sequences of gas discharge phenomena more or less already accepted as being associated with the generation of positive streamers both for uniform (section 3.1) and non-uniform (section 3.2) field gaps. A computer simulation model of the development of an active cathode region by the streamer arrival to the cathode is presented in section 4. The following section 5 discuss well-known gas discharge phenomena as negative corona TPs and instabilities of the high-pressure cathode regions which, however, are not still accepted by the gas discharge community as being associated with the positive streamer formation. Section 6 summarizes the discussions and conclusions presented in sections 2–5 attempting first to remedy the existing terminological misunderstandings and then to present an unified experimental and theoretical picture of the sequence of ionization events leading to the streamer breakdown.

2. Historical overview, experimental developments, and basic terminology

The sudden transition of laboratory air to a highly conducting state with a negative resistance phase termed the spark or complete gas breakdown [14, 15], was studied already in the middle of 18th century by Benjamin Franklin, who had demonstrated that a laboratory spark and lightning were of common nature [9].

The progress in vacuum technique enabled to ignite steady gas discharges at reduced pressures and moderate voltages, also often termed as 'breakdowns' [14]. In 1889, Paschen measured the minimum voltage that was necessary to ignite a discharge between two electrodes in a vacuum tube [16]. He found that the minimum discharge ignition voltage (the static breakdown voltage V_s) is a function of the product between gas pressure p and gap distance d and measured dependences $V_s = f(p \cdot d)$ nowadays known as Paschen curves.

In 1910, based on the extensive studies of low-pressure gas dischages by measuring the discharge currents by an electrometer and inductive balance, Townsend published his 'Theory of Ionization of Gases by Collision' [17] with the equation describing the observed exponential spatial growth of the ionization with the distance from the cathode attributing, however, the ionization by collisions to the impact of negative and positive ions. The following combination of Townsend's equation with the finding that the discharge current is mainly carried by electrons generated predominantly through the collision processes of electrons with gas atoms and molecules [18, 19] resulted in what is currently called the Townsend breakdown theory and in the well known Townsend equation based on the exponential development of current in a series of electron avalanche generations [20] linked through secondary-emission feedback to the cathode. The criterion for the self sustaining discharge resulting from the Townsend equation is that each electron avalanche produces at least one secondary electron at the cathode, so that the discharge is self sustaining:

$$\gamma(e^{\alpha d} - 1) \geqslant 1, \tag{1}$$

where d is the gap spacing, α is Townsend's first ionization coefficient and γ is the number of secondary electrons produced at the cathode per ionizing collision in the gap (Townsend's coefficient of secondary emission).

The Townsend theory has been very successful in explaining breakdown phenomena in uniform fields under various discharge conditions as, for instance, explanation of Paschen's breakdown curves, and effects of electronegative gases and cathode materials on the breakdown voltage. Following the pioneering works by Rogowski and Schumann [21, 22], in the 1930s and 1940s the ongoing development of experimental equipment enabled the experimental study of transient breakdown processes. By measuring cloud-chamber tracks of electron avalanches and interrupted sparks it was verified that at sufficiently high over-voltages the final spark breakdown occurs in 10^{-7} s or less [3]. Such fast spark breakdown was found to be due an extremely rapid ionization process requiring only a single large avalanche, rather than the slow cumulative action of a sequence of avalanches with the feedback to the cathode. This and others reasons to question the validity of the Townsend theory at higher pressures and larger electrode distances ($p \cdot d > 10^3$ Pa m) were analyzed in details by Meek [23]. As a consequence, the so-called streamer mechanism was proposed by Flegler and Raether [24], Loeb [25] and Meek [23] particularly to explain the fast single-avalanche breakdown observed in highly overvolted gaps at near atmospheric pressures, where the pulsed voltage magnitude is exceeding some 100% of V_s. In the

1950s the availability of high-speed oscilloscopes and photomultipliers enabled Amin [26], Anderson [27], and Hudson and Loeb [14] to make the first observations of the full sequence of events leading to the spark breakdown, where during the first phase of breakdown thin plasma channels the so-called primary streamers were formed.

In the past four decades, the development of both streak and gated intensified CCD cameras [28–31] has enabled such phenomena to be observed with a temporal resolution on the order of nanoseconds. The results obtained mainly in short positive point-to-plane gaps in air indicate that a spark breakdown at near atmospheric pressure is always preceded by the formation of a cathode-directed primary streamer propagating with the velocity in the range 10^7–10^8 cm s^{-1} and its arrival to the cathode. As studied in details [32] and reviewed for example in [33] the primary streamer head propagates as a luminous spot of the diameter in the range 10^{-5}–10^{-3} m. The streamer diameter, or parameters of its 3D structure in general, is typically evaluated from CCD camera images and, consequently, the results can be affected by resolution and sensitivity of the optical apparatus used. Moreover, different measures are used for its quantification—e.g. FWHM of the luminous fingerprint, 10%-to-90% of pixel-by-pixel summation, electrodynamic radius etc [34–37]. Other approaches investigated the quantification of the relation of the streamer diameter parameter to other qualities of the propagating discharge [36, 38, 39]. In view of the accuracy of both experiment and theoretical models used, the sometimes claimed agreement between the measured and computer simulated streamer diameters might be still not sufficient, as it was shown especially for lower pressures in [35].

Other developments have taken place in the application of modern sophisticated spectroscopic techniques and the interpretation of their results for investigation of various phenomena occurring during the streamer formation and propagation [40–42]. For example, to study repetitive streamer phenomena with high spatial and sub-nanosecond temporal resolution, correlated single photon counting techniques have been used, where the weak photomultiplier signals from the space, time, and spectrally resolved light from millions of streamer pulses were accumulated [43–47], also in two-dimensions (2D)48, 49]. Nevertheless, the transient feature and the small dimensions still make some basic streamer parameters difficult to be accessible to the experiments.

Because of currently increasing availability of methods and oscilloscopes allowing measurements of current pulses with a sub-nanosecond rise time, large amount of information on the streamer phenomena have been obtained by measurement of the currents induced by the fast streamer phenomena in a large variety of discharge gaps and probes [50]. The simplest way called by Raether 'electric method' [51] to measure a streamer current is to use a low-inductance measuring resistor in series with a homogenous field gap, or Rogowski coils for the time resolution not less than ~1 ns. However, using parallel plane electrodes the measured rise time is critically limited by a high gap capacitance, even for relatively small electrode areas. Moreover and unfortunately, the difficulty to correctly measure and interpret the streamer-induced currents with sub-nanosecond temporal resolution has been often ignored by the workers in the field of gas discharges. At measurements of fast current signals induced by the streamers, it must be taken into account that the nano- and sub-nanosecond time resolution is provided only using probes with small receiving areas, as sectional electrodes [28, 46, 52–55], and using the input wave impedance equal to the wave impedance of a coaxial cable through which signals are transmitted to an oscilloscope. Moreover, as discussed in more detail in section 3.2, particularly for non-uniform field gaps the interpretation of measured current waveforms is complicated by a complex interrelation between conduction and displacement currents which are produced by propagating streamers in such probes [13, 28, 51, 56].

Along with the advances in experimental techniques, starting in the 1970s the fluid numerical modeling of the primary streamers development and propagation has been increasingly utilized [57]. Soon, also first attempts [58, 59] were made to use the more advanced kinetic approaches for simulations of highly non-equilibrium, nonlinear, and non-local conditions of a typical primary streamer formation and propagation. Using faster and more accurate algorithms the computer simulations become essential tools that can be used in synergy with the experiment to increase our fundamental understanding of the streamer-related phenomena.

At larger inter-electrode gaps in air, where secondary electrons from the cathode are too delayed to play any role, the positive streamer propagation is critically dependent on the presence of seed electrons ahead of the streamer tip [60–63]. However, the computer simulations by Kulikovsky [64] and Pancheshnyi [38, 65] taken together with the current experimental results in [65–68] quite persuasively indicate just a weak sensitivity of the streamer characteristics to the density of the seed electrons. The weak dependence of streamer characteristics is due to the fact that the effective parameter that appears in simple streamer theories is actually a logarithm of the seed electron density [69, 70]. As stated by Kulikovsky [64]: *'In a weak field the role of photoionization is to provide at least one seed electron ahead of the tip. Further multiplication of charges occurs due to collisional ionization'*. It appears that in many real situations the limiting factor for the primary streamer formation and propagation is rather too high ionization of the background gas [71, 72]. According to Wormeester *et al* [67] and Celestin *et al* [73] the photoionization is the primary source of seed electrons in air except for high background ionization above ~10^{10}cm^{-3}. Consequently, the rigorous definition of primary streamers as *'Subset of ionizing potential waves propagating in initially unionized gas'* [59, 74] is lacking practical relevance. This fact can be documented, for example, by the results indicating that the so-called plasma bullets can be successfully interpreted as a positive streamer guided by a helium plasma jet, whereby the streamer dynamic is not critically affected by the preionization density [75, 76]. Also, it is generally accepted that large-scale sprites propagating at a high background electron density in lower ionosphere are physically similar to

small-scale streamer dischargers in air at atmospheric pressure [77, 78].

Another controversial issue of a significant practical importance is the criterion for streamer-initiated breakdown. In a historical context it should be noted that some of the above mentioned discrepancies between the breakdown experiments and the Townsend theory sumarized by Meek [23] were later resolved [79]. Also, even when the Townsend theory yields the criterion for establishing a low-current space charge free Townsend discharge, it is often used as a working breakdown criterion for the onset of streamer coronas and complete breakdowns in non-uniform fields [13, 80]. This quite surprising fact is clarified by the excellent but often overlooked work by Hodges *et al* [20], where the 'pure' Townsend and the 'traditional' single-avalanche streamer mechanisms are just limiting cases accounted for the spark breakdown. In fact, as it will be discussed in more details later, the breakdown criterion, if considered correctly in terms of the breakdown probability, does not depends on the mechanism of streamer propagation, but rather on the conditions under which the space-charge initiating the primary streamers is generated: Generally, a streamer starts when the charges that appear on the surface of a streamer-initiating plasma become able *'to shield the interior* (that) *unavoidably enhance the electric field over a limited region just outside of the streamer'* [81]. Such streamer-initiating plasma region can be generated not only by a single 'critical' avalanche as considered by the traditional streamer theory, but particularly in non-uniform fields more often by a sequence of avalaches linked by a secondary electron emission from the cathode or photoinization [82–85].

3. Streamer breakdown

Since the time when the streamer theory was first postulated for the single avalanche spark breakdowns in the over-volted uniform field gaps, being driven both by the advance in fundamental discharge physics and applications, considerable efforts have been devoted to examining how it can be generalized and applied to a wide range of experimental and practical conditions, such as different gases and pressures, electrode geometries, over-voltages, etc. Nevertheless, despite decades of intensive research efforts driven both by the advance in fundamental discharge physics and applications it appears that existing extensive scientific and technical literature on the streamer breakdown of centimetric gaps suffers from a lack of consensus on several central issues [60, 80, 86]. As a consequence, a satisfactory understanding of the sequence of events related to the streamer breakdown from the initiation, by say a single electron, to the stage where arc current of many amperes flows in the gap, remains a challenge for the future. To get an overall picture of the streamer breakdown phenomena in the short gaps, where the breakdown typically evolves without the formation of a leader [87, 88], in this section we will attempt to summarize and distill both older and contemporary findings and knowledges in the field.

For the sake of brevity and simplicity, we will concentrate mainly on the DC, impulse, and low frequency prebreakdown and breakdown phenomena in near-atmospheric pressure air and nitrogen. Nevertheless, since the streamer discharges are in general very robust against changes of gas composition [66], we believe that many results and conclusions presented will also be applicable, perhaps with some modifications, to high-pressure gas discharges in other gases and gas mixtures. In line with Kunhardt [89] we will assume that the basic breakdown processes, including the streamer phenomena, and their contribution to the development of breakdown are in general common to both DC and pulsed breakdown. Moreover, we will not consider the discharges generated in atmospheric pressure air and other gases by application of high voltage pulses with a nano- or subnanosecond rise time, where the breakdown phenomena are significantly effected by beams of fast electrons [90–95].

An excellent starting point is the concept presented by Marode in figure 1, [96], illustrating significant similarities between the sequences of events leading to the streamer-initiated breakdown in the short parallel-plane and positive point-to-plane gaps.

3.1. Streamer phenomena in uniform fields

3.1.1. Single avalanche streamer breakdown. The figure 1(b) illustrates the already mentioned 'classical' single-avalanche streamer mechanism proposed in the 1930s and 1940s to explain the already mentioned fast breakdown observed in cloud chamber experiments in the parallel plane gaps under high impulse conditions. In the experiments often labeled as 'single electron initiated' [100] the single avalanche starts from an electron emitted from the cathode. Till the net charge in the avalanche head is not sufficient to significantly distort the external electric field, the avalanche grows exponentially, and its head moves with the electron drift velocity in a concentrated path due to the low lateral diffusion of electrons at high pressures. Raether [101], still based mainly on the early cloud chamber results and approximate calculations of the space charge, concluded that the avalanche growth was weakened after the avalanche reaching around 10^6 electrons and stopped reaching a 'critical size' N_{ecr} at around 10^8 electrons, being transformed to a region of streamer-initiating plasma at a distance $x_c = \ln(N_{ecr})/\alpha$ from the cathode.

If the gap over-voltage is not too large, this can occur in the anode vicinity resulting there in the initiation of a cathode-directed streamer, or if the gap and voltage are large enough, the avalanche-to-streamer transition can already take place quite far from the anode. In the second case, as illustrated in figure 1(b), both cathode and anode streamers directed are initiated [102]. The single avalanche-to-streamer transition occurs due to the generation of new avalanches initiated say through photoioniziation, joining with the head of the primary 'critical' streamer-initiating avalanche to form a rapidly developing streamer front propagating to the cathode, and eventually also to the anode, which have come to be referred to as the positive and negative primary streamers. Since the streamer velocity is much higher than the electron velocity v_e

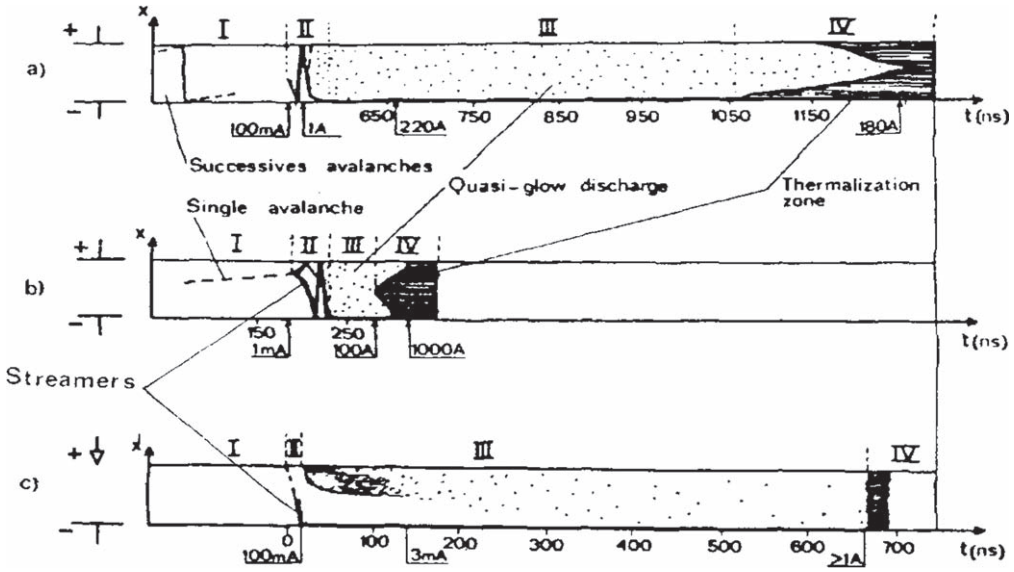

Figure 1. Comparison between typical streak photographs of the spark formation in different cases according to Marode [96]. (a) Uniform field gap: nitrogen, pulsed gap with small overvoltage (7.55%), generation mechanism, $p = 300$ Torr, $d = 2$ cm (after Doran in [97]), (b) uniform field gap: nitrogen, pulsed gap with high overvoltage (35%), streamer mechanism, $p = 300$ Torr, $d = 2$ cm, (after Koppitz [98] and Chalmers and Duffy [99]), (c) non-uniform field gap: air, DC potential, $p = 760$ Torr, $d = 1$ cm, point radius 100 μm (after Marode [28]). The picture is taken from [96].

in a Laplacian field, the upper limit of the formative time of the streamer breakdown is often considered [10] as:

$$t_{\mathrm{d}} \leqslant \frac{\ln N_{\mathrm{ecr}}}{\alpha v_{\mathrm{e}}}. \tag{2}$$

For an avalanche started from the cathode, this transition corresponds to a value of $\alpha \cdot d$ of about 20 in the undistorted applied field. This empirical criterion $\alpha \cdot d > 20$, nowadays known usually as the Raether–Meek criterion for streamer breakdown [102] is widely and successfully used for the impulse breakdown in highly overvolted uniform field gaps. Note that starting from the work by Kunhardt and Tzeng [59] many computer simulation works try to explain in details the plasma processes related to the single avalanche-to-streamer transition, which is more complex and less amenable to experiment than the subsequent positive streamer propagation already briefly discussed in section 2. A detailed theoretical discussion of the single avalanche to streamer transition including the resulting breakdown criteria is presented, for example, in a recent study by Rabie and Franck [103].

As illustrated in figure 1(b), in a single electron initiated breakdown at the high over-voltage values, the Phase II is starting by the single avalanche-to-streamer transition, and it is terminated when a cathode spot of high electric field and high positive-ion densities is established by the positive streamer arrival to the cathode. As seen from figure 1(b) the fast cathode spot establishment is followed by a complex sequence of secondary streamers. As suggested for example by Llewellyn-Jones [104], the arrival of the streamer to cathode can initiate the secondary streamers by *'a burst of electrons to give a high field running back along the track'*. The subsequent bridging of the gap by secondary streamers results in the establishment of a short-duration filamentary 'quasi-glow discharge' (see Phase III in figure 1(b)) followed by a fast glow-to-arc transition (IV) that greatly increases the conductivity of the gas if the power supply can deliver the arc current above some amperes.

3.1.2. Multi-avalanche streamer breakdown. The above discussed single avalanche streamer mechanism of the highly-overvolted gaps illustrated by figure 1(b) constitutes the fundamental characteristic of the 'classical' streamer concept of breakdown generally accepted by the workers in the field of gas discharges, and taught in standard textbooks and reviews on the gas discharge physics [9, 105]. However, as reported by Hudson and Loeb already more than half of century ago [14] for parallel-plane gaps: *'The filamentary spark, except at high, short impulse overvoltage, is now recognized as being preceded by a low-order self-sustaining discharge. These lower order discharges are at times nearly imperceptible and at other times obvious as a Townsend glow discharge in uniform fields ...'* (see also [13], discussed in section 6).

Such low order Townsend type discharges are illustrated in figure 1(a) that is based on the results of an excellent and still very valuable study of the multi-electron initiated multi-avalanche breakdown by Doran [97]. As it is characteristics for a Townsend discharge, the ionization during Phase I initiated by 'a pulse of some 400 electrons' is due to the superposition of several generations of electron avalanches linked by the secondary electron emission. It is interesting to note here that Marode in figure 1(b) assigned the single electron initiated breakdown in figure 1(b) to the 'streamer mechanism', while the multi-avalanche initiated breakdown in figure 1(a), despite the evident formation of streamers (see, also discussion to follow), as a 'generation mechanism'. Such a very common but misleading 'streamerless' breakdown

terminology can be exemplified by the following claim by Cavenor [106]: *'The filamentary spark channel, resulting from the electrical breakdown of a gas, generally forms in one of two ways. At voltages close to the minimum breakdown potential the spark channel has been shown to develop from the constriction of the diffuse glow discharge formed from the superposition of many generations of electron avalanches. At large over-voltages, however, single avalanches have been observed to develop into luminous conducting filaments, called streamers, which completely bridge the electrode gap within the transit time of the initial avalanche'*, and more recently by the claim regarding the streamer formation in non-thermal atmospheric pressure gas discharges in general *'The formation of a streamer requires the electric field of the space charge in the* (single) *avalanche to be of the order of the external field'* in [105]. Unfortunately these works, as well as many textbooks and reviews on gas discharge physics ignores the following facts and opportunities stated already by Loeb in 1951 [107]: *'Thus, spark discharges in uniform fields set in at thresholds for low order Townsend discharges by creating space charge field distortions. These distortions increase to the point where avalanches reach streamer-forming proportions in middgap, thus yielding sparks as streamer-type breakdown. ... The physicist must, therefore, reconcile himself to the paradoxical situation of a streamer breakdown mechanism for spark in uniform fields with a threshold which is set by the conventional Townsend criterion and not by that of Meek and the writer and of Raether. If this is done, practically all of the difficulties of the past are reconciled in a single consistent sparking theory.*' In this context the reader is referred again to the paper by Hodges *et al* [20], where this long-standing problem is treated correctly in terms of *'a unified* (statistical) *breakdown theory for which the Townsend and streamer mechanisms are limiting cases'*.

Turning back to Doran's results [97] illustrated in figure 1(a) who described the Phase II in terms of the Townsend ionization mechanism: Following the Stage I initiated by a pulse of some 400 electrons, at the beginning of the Stage II *'The results indicate a well defined luminous front which is first observed in the midway between the anode and cathode moving towards the cathode with a velocity which increases from* $5 \times 10^7\,\mathrm{cm\,s^{-1}}$ *to* $10^8\,\mathrm{cm\,s^{-1}}$. *This stage corresponds to the motion of the contracting leading edge of the discharge shown in the intensifier shutter photographs. On its arrival at the cathode a flash appears at the surface of the electrode, coinciding with a marked kink in the current curve* (see figure 2). *From this short duration flash at the cathode another front is launched, travels towards the anode at a velocity of* $2 \times 10^8\,\mathrm{cm\,s^{-1}}$ *and this in turn initiates a further wave which returns towards the cathode with a slightly higher velocity.*' Figure 2 shows the 'marked kink in the current curve' measured by Doran together with the results of early computer simulations by Davies *et al* [108], who however termed the luminous front arrival resulting in the short duration flash at the cathode as the 'cathode streamer arrival'.

As illustrated in figure 2, using several approximations, as arbitrary changing the discharge radius according to

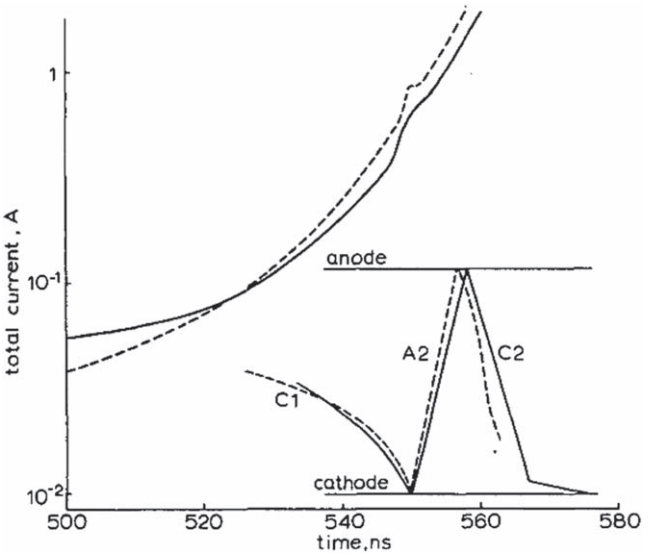

Figure 2. Schematic representation of the experimentally measured (——, according to [97]) and theoretical (- - - -) discharge currents and luminous fronts in conditions identical to figure 1(a). Taken from [108].

Doran's data [97] and neglecting the space charge effects, Davies *et al* [108] claimed to succeed (see figure 2) in simulating the current kink due to the positive streamer arrival and the development of subsequent secondary streamers. Nevertheless, a later attempt to simulate 'multi-electron initiated' breakdown by Doran in 2D and incorporating the effects of space-charge distortion made also by Davies [109] was not successful since *'the calculations eventually break down as the cathode streamer approaches the cathode because of numerical instabilities.*' From the literature as, for example, the recent review by Liu and Becerra [110], the current calculations still tend to breakdown as the streamer approaches the cathode because of numerical instabilities. As a consequence, a satisfactory computer simulation fluid models describing in details all stages of the streamer breakdown in uniform field gaps, as illustrated in figures 1(a) and (b), still remains a challenge for the future. Moreover, as discussed in section 3.2.1 and in details shown in section 4, the fluid models assume more or less equilibrium of electrons with the electric field, which is not always true, particularly for electrons in the strong field in the streamer head approaching the cathode, where the electrons can gain more energy from the electric field than they lose by collisions.

The streamer mechanism is also responsible for abrupt ionization in DBDs which are widely used as plasma sources both in technological applications as well as fundamental research fields. Although the detailed discussion of the streamer phenomena connected to DBDs is beyond the scope of this review, we address some important issues of general interest later in the appendix of this manuscript.

In contrast to the above discussed low-overvoltage multiavalanche-initiated (streamer) breakdown, the special 'multiavalanche pulsed discharge' (termed according to [10, 100]) can be generated in pre-ionized highly-overvolted

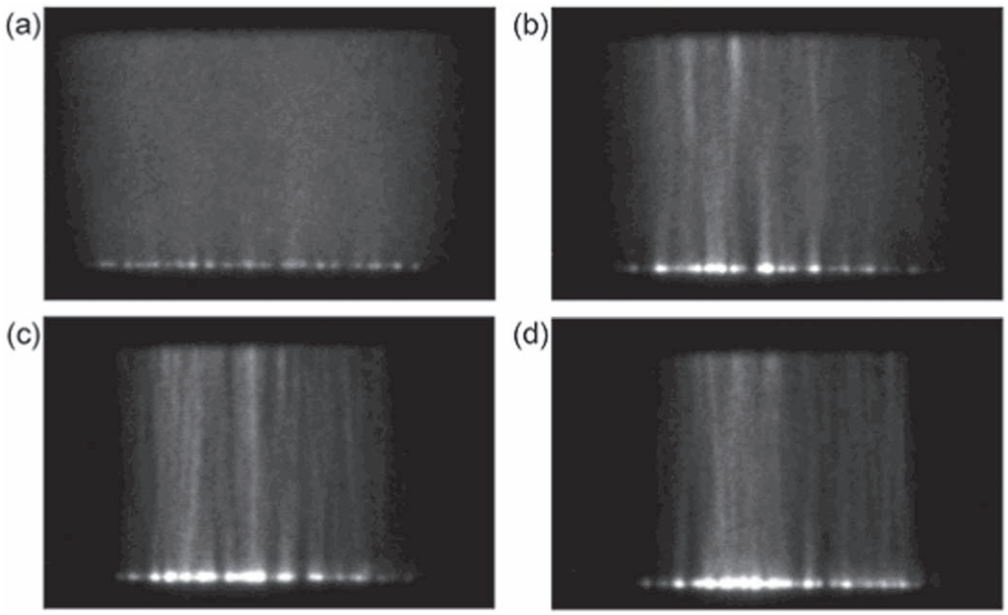

Figure 3. The formation of cathode spots in conditions simulating a TEA laser in HCl/Kr/Ne with partial pressures of (1/100/4899) mbar, impulse voltage of approximately 25 kV and $d = 2$ cm. (a) 100, (b) 200 (c) 300, and (d) 400 ns after the discharge onset. Taken from [114].

gaps at the condition $\ln N_{\mathrm{ecr}}/\alpha \ll d$. Such situation of great practical interest arises when preionization of laser gases is used to generate pulsed volumetric glow discharges at gas pressures greater than 1atm.: starting the avalanches in a pre-ionized highly over-volted gap by a large number of pre-ionization electrons, the heads of primary avalanches start overlapping before the space charge field becomes comparable with the applied electric field [111–113]. The pre-ionization will prevent the already mentioned situation [107] *'where avalanches reach streamer-forming proportions in middgap, thus yielding sparks as streamer-type breakdown'*, i.e. a sufficient pre-ionization can prevent the formation of a streamer initiating plasma by smoothing out the local gradients of the space charge field. In this way, the electron density can grow uniformly in the discharge volume and a homogeneous glow discharge with a high-field electron-depleted cathode region can be established without streamer formation [111]. Nevertheless, the praxis show that even under such optimized conditions in transversely excitedatmospheric (TEA) lasers an undesired plasma filamentation occurs, which is triggered by cathode spots quickly (∼10–100 ns) developing in the initially laterally homogeneous cathode sheath. It is interesting that even when the cathode spot formation is caused by a stochastic electron emission from randomly distributed cathode surface imperfections, the spots are often regularly distributed at the cathode surface [114].

According to computer simulations by Smy and Clements [115] such instability occurs because the anode-side of the established cathode sheath acts effectively as a virtual anode, and finaly *'the sheath can collapse catastrophically with an accompanying decrease in its impedance of many orders of magnitude'*. Belasri *et al* [116] based on their 1D computer simulations suggested that a streamer collapse of the cathode sheath was due to an anode-directed streamer formation in the sheath. According to the 2D computer simulations results by Černák *et al* [117], where the sheath collapse was initiated by a 10 ns burst of electrons from a typical cathode emission site, such electron emission forms a space charge distortion on the cathode-faced surface of the bulk plasma, i.e. on the virtual anode. In agreement with the extensive and still unique experimental results by Makarov *et al* [118, 119] and contrary to the model by Belasri *et al* [116], the space charge distortion propagates not from the cathode, but from the virtual anode taking the form of a positive streamer-like ionizing wave. At the streamers arrivals, similarly as in figures 1(a) and (b) cathode spots like those seen in figure 3 are formed. In agreement with experimental results by Makarov *et al* [118, 119] and Drieskamper *et al* [120] the simulations in [117] indicate that the cathode spot formation is an extremely rapid process in the nanosecond range associated with a positive streamer formation in the narrow cathode region, which can produce local concentration of current in the cathode sheath leading to the subsequent undesired glow-to-arc transition. Unfortunately, the calculations by Černák *et al* [117], similarly as those by Davies [109] and many others, broke down as the cathode streamer approached the cathode so that the subsequent formation of a cathode spot like those seen in figure 3 was not treated in details.

Nevertheless, the authors suggested that their results (see figure 4) taken together with the experimental results by Makarov and Bychkov [119] provide a base for unification of the initiating plasma-to-arc transition that occurs in pulsed high-pressure XeCl laser discharges into a general class of streamer breakdown phenomena. Due to the practical interest, the discussed works were done in conditions similar to those in UV-preionized XeCl lasers. Thus it is worthwhile to note that the results on breakdown formative time as a function of electric field in preionized pulsed air gaps can be found in

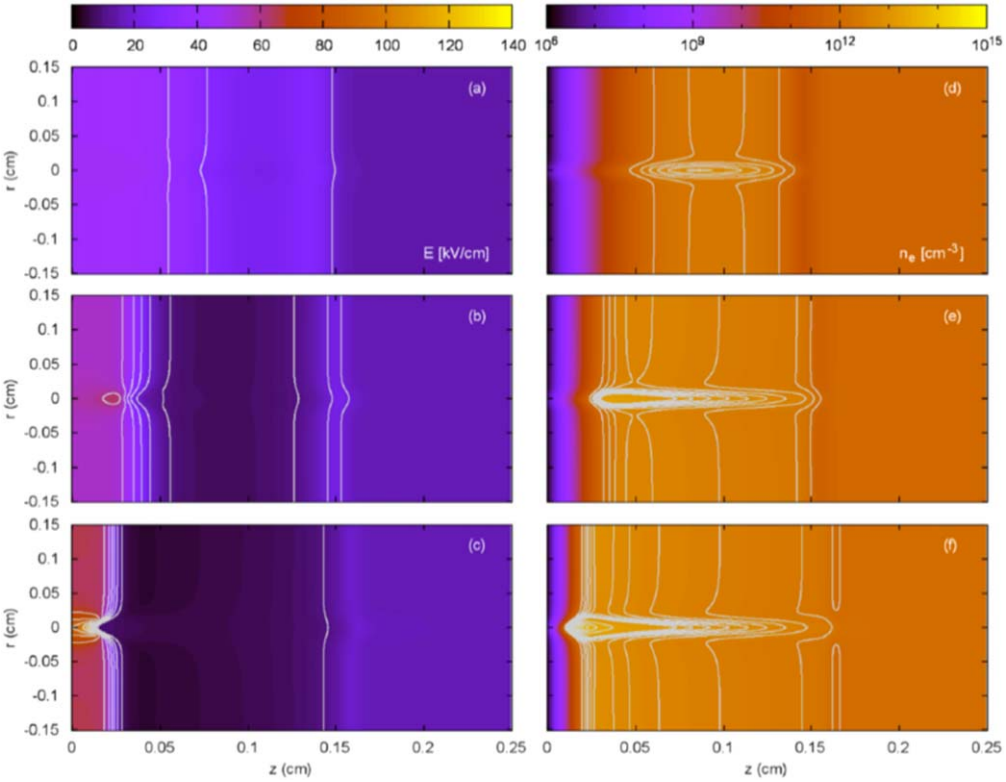

Figure 4. Simulation results of the positive streamer formation in the cathode region of a pre-ionized TEA discharge in neon gas at 3 bar pressure. Electric field (a)–(c) and electron density (d)–(e) at $t = 27$ ns, $t = 28$ ns and $t = 29$ ns. The isocontours of density are taken from 1×10^{12} cm^3 to 1×10^{13} cm^3 with a space between two isocontours of 1×10^{12} cm^3 and from 1×10^{13} cm^3 to 1×10^{14} cm^3 with a space between two isocontours of 1×10^{13} cm^3. The lowest isocontour of electric field is 10 kV cm^{-1} and the highest is 120 kV cm^{-1}, the space between two isocontours is 10 kV cm^{-1}. Taken from [117].

[121, 122]. Also, results by Baksht *et al* [123] on diffuse glow discharges in air and N_2 preionized at 1atm. by run-away electrons generated by the discharge itself correspond well with the work by Makarov and Bychkov [119] in Ne–Xe–HCl excimer gas mixture at pressures approximately 2 atm.

3.2. Streamer phenomena in non-uniform fields

In non-uniform field gaps the streamer initiating plasma is generated in a close vicinity of the high field electrode, and the streamers then can propagate farther away into the gap where the field is typically too low for streamer initiation, but high enough for streamer propagation due to its own space charge field. Figure 5 illustrates typical picture of such phenomena for positive and negative point-to-plane gaps in ambient air fed by voltage pulses with the rise times on the order of ~10 ns [32].

In electronegative gases (see figure 5) the streamers can propagate and cross point-to-plane gaps for a significantly wide range of applied voltages generating a partial breakdown without triggering a spark. Similarly to the breakdowns in highly-overvolted uniform-field gaps illustrated in figure 1(b), when the streamer is initiated by a single critical avalanche, the full breakdown in non-uniform field gaps is also often termed the 'streamer breakdown' [124, 125]. This, however, contradicts to the fact that, as discussed below, the streamers in figure 5 are not initiated by a single 'critical' avalanche and, consequently, the 'streamer breakdown criterion' by Raether and Meek is not fulfilled there.

In attempting to provide an unified model for the streamer breakdown phenomena it is useful to use also the term 'corona discharges', even when the terminology is also somewhat confused:

For example, according to Goldman *et al* [126] the corona is a low-current discharge characterized by a faint visual glow in the high-field region: *'A corona is self-sustained electrical gas discharge, where the Laplacian electric field confines the primary ionization process to the regions close to high field electrodes or insulators'*. Thus the authors included in their definition also 'DBD coronas' formed close to insulator surfaces, and termed the discharge with the streamers propagating farther away into the gap like those in figure 5 as the 'streamer (bipolar) conduction coronas'. The definition by Kogelschatz and Salge [127] is more general and more convenient to be used in the following discussion: *'Corona discharges are self sustained gas discharges typically operated in air at atmospheric pressure between metal electrodes. At least one of the electrodes is of a geometric form which causes locally high fields. Common configurations are pointed electrodes facing a plane,* ...etc. *When the voltage is raised in such a configuration current starts to flow at corona onset and increases until the potential for spark is reached. This intermediate range of corona activity is referred to as a partial breakdown of the gap. The corona is characterized by*

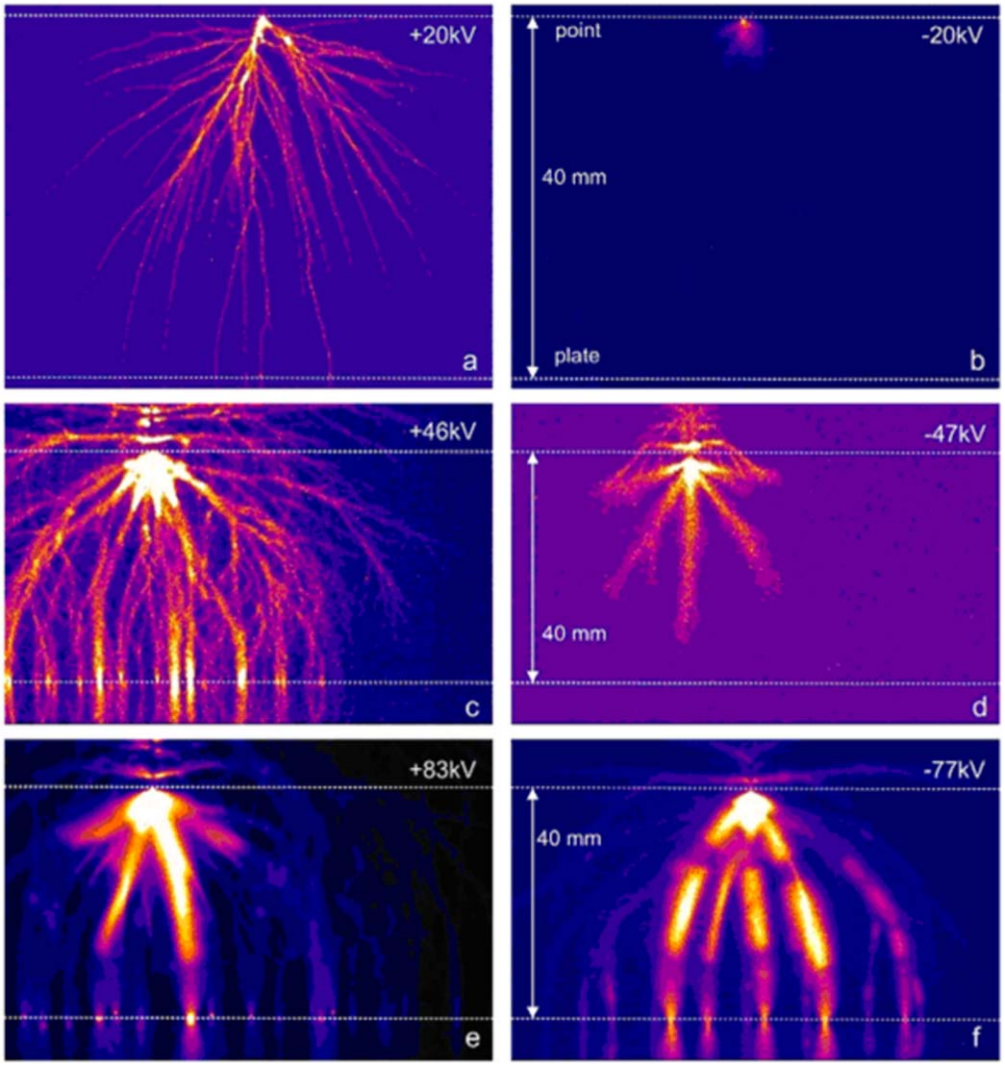

Figure 5. Time integrated photographs of positive (left column) and negative (right column) streamers in a 40 mm gap in air at 1 bar for different pulse gap voltage values according to [32].

a faint visual glow in the high-field region occasionally accompanied by luminous streamers propagating toward the other electrode.'

3.2.1. Streamer phenomena in non-uniform fields with highly stressed anodes. A detailed understanding of the positive streamer initiation, propagation, and its arrival to the cathode forming an active cathode spot, are principal for the general understanding of the streamer breakdown. As a consequence, the great majority of the study focused on these pre-breakdown events was done in the positive point-plane gaps, where the whole sequence of events leading to the breakdown, is better discernible than in the uniform field gaps, and thus more amenable to both experimental and theoretical studies.

Loeb [60] was the first who commented on *'observed fine electric blue streamers darting outward from the point which indicated a progressive projection of very high field regions from the positive point into the gap'* (see figure 5) and *'pointed out that these streamers constituted a new type of breakdown process.*' Even when this phenomenon was considered by Loeb as a 'new type of breakdown' in praxis it turned out that ambient air streamer coronas and breakdowns in positive point-to-plane gaps are widely used for basic studies of the streamer phenomena in general [28, 46].

A considerable amount of experimental, theoretical, and numerical effort [128–131] has been devoted to the understanding of the positive streamer initiation near the anode tip in ambient air:

According to Gosho and Saeki [132], the discharge in electronegative gases is triggered by electrons detached from negative ions arriving to the high-field region near the anode. Subsequently, following a pre-corona sequence of avalanches [82], a positive streamer is initiated close to the anode. Later this initial discharge stage was studied in more details by Laan and Paris who found that [84] *'In a divergent field the streamer formation is preceded by the accumulation of space charge, i.e. it has a multi-avalanche nature.*' and *'A streamer starts when the space charge density reaches a critical value in a spatially localized region.*' This is in agreement, for

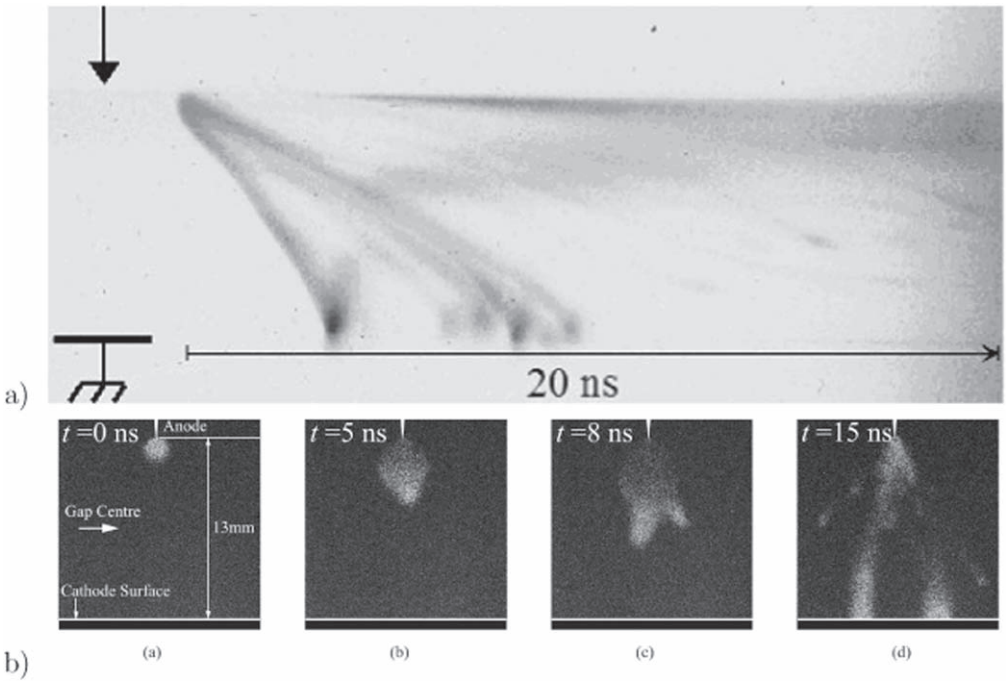

Figure 6. Streak camera record in a 2 cm ambient air gap with an anode radius of 50 μm. The applied voltage and streak are 36.8 kV and 20 ns, respectively [140]. ICCD camera records made in a 1.3 cm ambient air gap with an anode radius of 80 μm, applied voltage of 35 kV at exposure times of 2 ns, part (b) taken from [141].

example, with the results of computer simulations [37, 133] indicating moreover that the density of the initial seed electrons hardly influences a positive streamer initiation and propagation a positive poin-to-plane gap. The results in [130, 134] also envisage the streamer initiation as a detachment of the ionization layer from anode surface.

This is in general agreement with the description of the streamer initiation by Nijdam *et al* [135]: *'The discharge starts with a small ball of light around the needle tip that was called the initiation cloud. This ball expands and forms a shell; this shell can be interpreted as a radially expanding ionization front.*' Depending on the impulse voltage rise time and magnitude, and gap length, the expanding shell breaks up into a single or multiple streamer heads. This picture is in general agreement also with the experimental results by Lowke and D'Alessandro [136]. They found that the onset of positive corona in ambient air occurs in a multiavalanche process for avalanche sizes above 10^4, that is significantly lower than the 'critical size' of 10^8 that would be expected from the Raether–Meek streamer criterion. This conclusion is in line, for example, with the theoretical consideration by Warne *et al* [80] that *'for increasing non-uniformity, the results for the corona and spark branches of the breakdown characteristics are shown inconsistent with a breakdown criterion solely based on either the Townsend or streamer mechanisms.*'

Unfortunately, despite the existing experimental data some of the current simulations still have attempted of to treat such positive streamer initiation not in terms of a streamer initiating plasma ('initiating cloud') generated by many avalanches, but 'traditionally' in terms of a critical single avalanche or of a chain of critical size avalanches [137–139].

The several streamers propagating from the 'initiating cloud' towards the cathode with speeds of the order of 10^8 cm s^{-1} are well discernible in the streak camera record by Bessieres *et al* [140] in figure 6(a) corresponding well with figure 6(b) taken in similar experimental conditions [141] and with the schematic picture in figure 1(c).

The formation of the secondary streamer starting from the anode immediately after the primary streamer arrival, firstly discussed in detail by Sigmond [142], can be properly seen in the figures 5(c), (e) and 6(a).

From figure 6, it is apparent that several streamers developed from the streamer initiating plasma and reached the cathode at different times. The 'flashes of light' [143] at the streamer arrivals are well discernible in figures 5(a), (c), (e) and 6. The streamer arrivals led to the flash of light and the formation 'more or less spherical cathode spots', as well as the re-illumination of the primary streamer channel corresponding to the secondary streamer launching are very well documented also, for example, in [32, 144]. Nevertheless, the secondary streamer formation due to the primary streamer arrival to the cathode remains somewhat obscure, apparently because of an incomplete understanding of properties of the cathode spot formed by the primary streamer arrival. For example, Suzuki [145] claimed that:*'After the primary streamer crosses the gap, a return ionizing wave moves from cathode to anode. This ionizing wave of potential gradient comes from the photoelectrons liberated by the light from the primary streamer tip and from the high field between primary streamer tip and cathode.'* However, in the fast streak-camera experiments by Bessieres *et al* [140], such as that shown in figure 6, the authors failed to observe the return ionizing wave proposed by Suzuki. According to them (see [140]), figure 6

'shows that the cathode spot formation seems to precede the secondary streamer start but the time delay between the two phenomena is too short to be measured on the streak. In fact, this time delay is consistent with the propagation time of an electromagnetic wave starting from the cathode toward the anode. This wave should be radiated as the electrical field in the head of the streamer tends to zero at its arrival at the cathode plane. Such a generated wave may be guided to the point by the streamer channel. This radiation phenomenon is considered to be close to the radiation of a monopole antenna.' The still not well understood formation of an active cathode spot by the streamer arrival, however, marks a turning point in the subsequent discharge development, since as found out by Kondo and Ikuta that *'almost of the electrons making the secondary wave luminous are fed through the cathode fall, and the ionization rate in the secondary wave column must be negligibly low'* [52]. Unfortunately, as discussed in details below, the current computer simulation models describe the cathode spot formation starting the secondary streamer only in the most superficial terms, see section 4.

The light reflection from the cathode surface, together with the small size and short duration of the cathode spots have made it too difficult to obtain their time- and space-resolved optical measurements. Fortunately, one of the advantages of short (∼1 cm) positive point-plane air gaps is that, using proper pulsed voltage and optimized electrode geometry, it is possible to minimize the generation of a multi-streamer bunch and the streamer branching [35, 146–148] like those seen in figures 5 and 6. This, as reported by Larsson [149], see figure 7, enables to measure the discharge current corresponding to the single streamer propagation in a virgin air and its arrival to the cathode with a nanosecond temporal resolution:

The figure 7 illustrates the voltage and anode current waveforms (in this case nearly identical with the cathode current) corresponding to the streamer breakdown measured by Larsson [149] in a rod-to-plane electrode configuration with a hemispherically tipped rod of 5mm radius and 1 cm interelectrode gap, where *'region 1 can be identified as the streamer propagation phase of the discharge and region 2 as the streamer*'s arrival at the plane electrode (cathode)', which are corresponding to the stage labeled II in the schematic streak camera record by Marode in figure 1(c). It is noteworthy that the fast rising (∼2 ns) current pulse formed by the streamer arrival to the cathode was in some 15 ns followed by a second current peak. Such double-peak structure was measured both in the pulsed voltage conditions [150], and in the below discussed repetitive corona conditions ([151] see figure 4 there, and [152]) using several different current measuring circuits. Thus it is apparent that the observed complex structure of the current pulse generated at the streamer arrival to the cathode hardly can be just an experimental artefact. Note also that the constant gap voltage during the stage 2 strongly indicates that the measured current maximum is not due to a charging of stray capacitance in the external circuit as suggested by Akishev *et al* [153].

The current signal in figure 7 is much better discernible than a not well pronounced current hump induced by the streamer arrival to the cathode in uniform field gaps (see figure 2) or in nearly uniform gaps [154], and reminds in the shape the current peak in figure A2 induced by the streamer arrival to cathode in DBDs. Since, as already mentioned earlier, it is difficult to obtain true temporal luminosity corresponding to the streamer arrival, the current signal like that in figure 7 can, as discussed below, provide important information on the complex nanosecond-scale phenomena at the primary streamer arrival to the cathode, subsequent cathode spot formation, and secondary streamer onset:

The streamer arrival to the cathode forming an active cathode region and signed in figure 7 by the sharp current peak on the discharge current waveform, critically determines the transition between the phases II and III illustrated in figure 1. This is confirmed, for example, by Marode [28] who claimed that in a short point-to-plane gap in air, the spark breakdown occurs only when the magnitude of the current peak generated by the streamer arrival exceeds a critical value, and that the current spike is due to an electron emission from the cathode.

In this context it is noteworthy that Loeb [143] observing the mentioned 'flashes of light' suggested that *'at a* (streamer head) *distance of a millimeter or less from the cathode, the intense ultraviolet radiation liberates a mass of electrons from the cathode'*. As a consequence a critical dependence of the current spike shape on secondary photoemission coefficient of the cathode is to be expected. Nevertheless, the experiments by Inoshima *et al* [147] comparing the current peak measured by Cu and CuI coated cathodes, as well as measurements by Johnson *et al* [155] revealed no significant dependence of the current peak like that in figure 7 on the cathode material. Alternatively, Nasser [156] obtained an experimental indication for a field electron emission occurring at the streamer arrival. In an attempt to test the effect of cathode properties Černák *et al* [150] compared the discharge current waveforms of a pulsed positive point-to-plane corona measured using a small cathode probe for an freshly polished unconditioned brass cathode with those obtained the well-conditioned cathode. The results shown in figure 8 confirm the insensitivity of the current peak on the cathode surface properties, but exhibit an unexpectedly strong effect that the cathode surface properties have on the subsequent glow-to-arc transition. The observed effect on the glow-to-arc transition is in some respect similar to that observed in TEA laser discharges [118, 157], and contradict the current physical description of the glow-to-arc transition in the conditions considered [125, 144], where the effect of processes in the cathode region created by the streamer arrival in the glow-to-arc transition is neglected. An interesting feature of the waveform 2 in figure 8 is the double peak structure A–B resembling that apparent in figure 7.

Černák *et al* [150] studied also the effect of a graphite coating on the cathode probe, that is known to have exceptionally low photoelectric yield and produces clusters of field emission sites. The graphite coating resulted in a

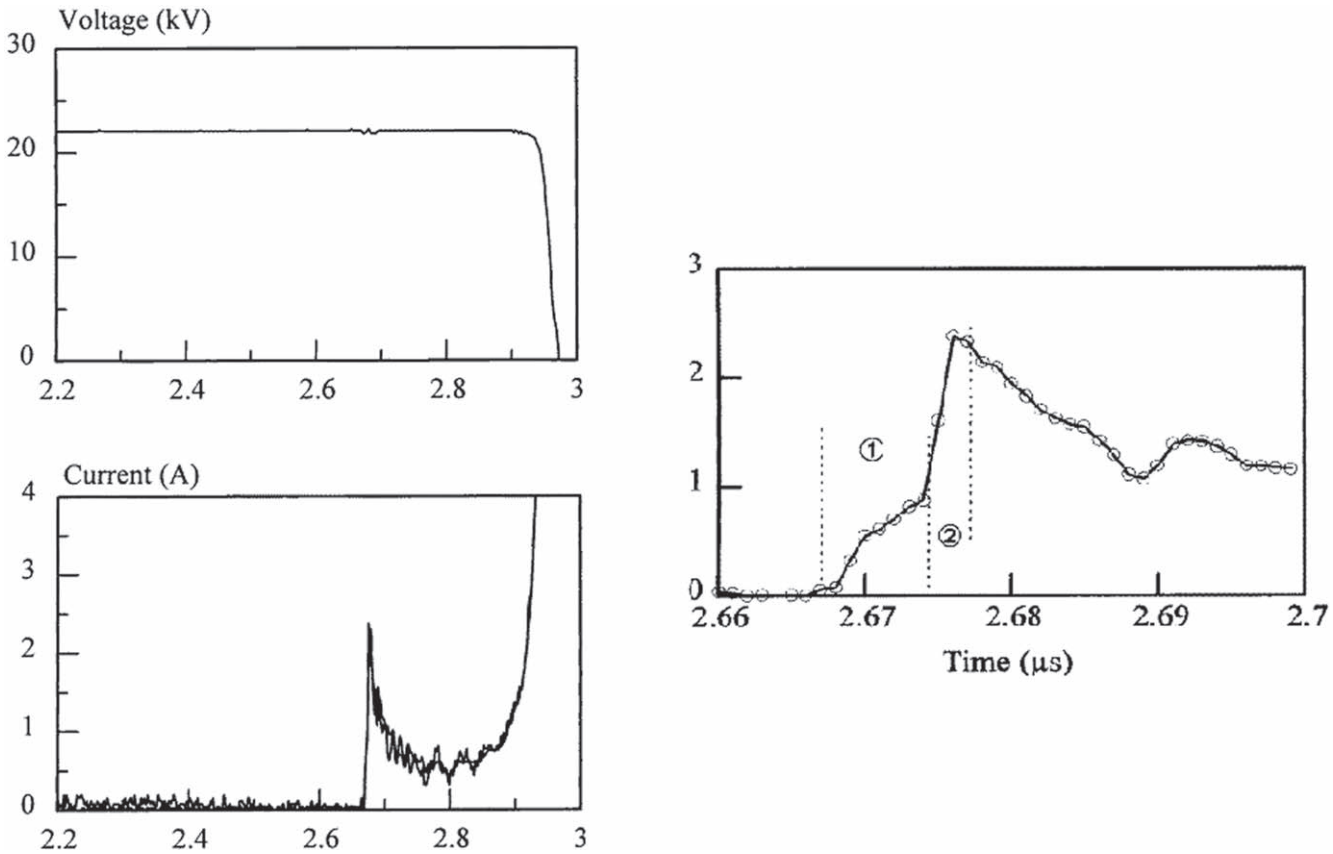

Figure 7. The gap voltage and the anode current waveforms corresponding to the streamer breakdown in a short ($d = 10$ mm) positive rod to plane gap in ambient air. The anode was a copper rod of 5 mm radius. Taken from [149].

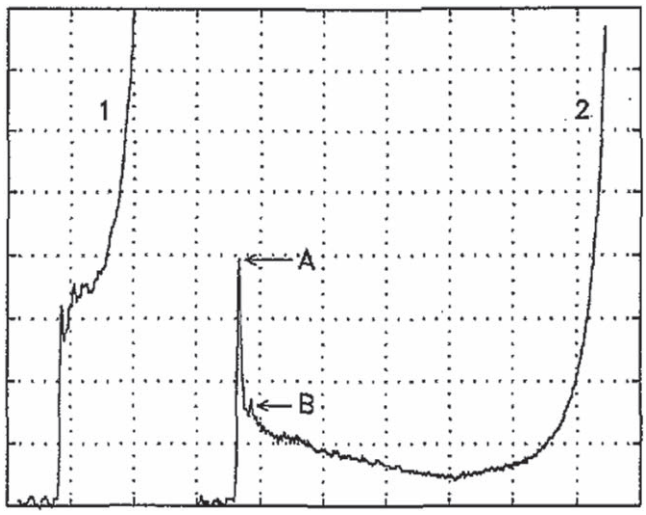

Figure 8. Comparison of the cathode current waveforms measured in a 1 cm positive point-to-plane gap in ambient air at a voltage of 20 kV. The current waveforms correspond to typical glow-to-arc transitions observed using the freshly polished brass cathode (curve 1) and the well-conditioned cathode (curve 2) surface at the same. (Scales: 400 mA and 50 ns per division.) Features of the waveform 2 denoted A and B are explained in the text. Taken from [150].

highly stochastic behavior of the current peaks induced by the streamer arrival and strong acceleration of the glow-to-arc transition like that in Curve 1 in figure 8 measured using the unconditioned cathode probe. Nevertheless, no relevant effect of the graphite coating on the pulse magnitude was observed. Note that the authors attributed the acceleration of the glow-to-arc transition observed using unconditioned and graphite-coated cathode surfaces to the existence of positive-streamer-like instabilities of the cathode sheath due to unstable and inhomogeneous electron emission from the cathode, as discussed in more details in section 5.2 (see also [158]).

The results by Černák *et al* [150, 158] exemplified in figure 8, call into question the 1D computer simulation models like those by Marode *et al* [159] and Naidis [125], as well as the more recent 2D simulations in [152, 160–162], where using the Neumann boundary condition, the cathode spot formed at the streamer arrival is considered to be just an electron source with zero internal resistance feeding the discharge during the glow-to-arc transition. For these works it is typical that *'The simulation of the streamer arrival to the cathode obviously depends on the boundary conditions used. This paper is not devoted to treat specifically the streamer hit to the cathode; only the secondary emission by the ion impacts is considered'* [161], and as noted also by Ducasse *et al* [163], there is a need for *'some specific analyses of the boundary conditions at the cathode plane.*'

To our best knowledge the only attempt to analyze in details the streamer arrival at the cathode and its transformation to the stationary cathode fall in a positive point-to-plane gap was done by Odrobina and Černák [56] for the discharge in nitrogen at 26.7 kPa. In the '1.5 dimensional' model the

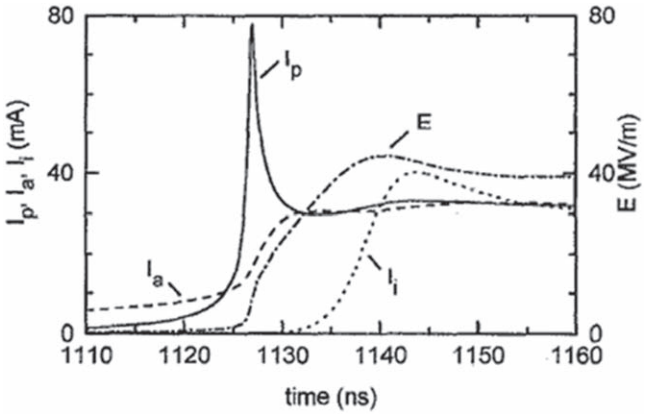

Figure 9. Time development of the total probe I_p, anode I_a, and conductive probe I_i currents simulated for the streamer arrival to a 4 mm—diam. cathode probe in a short ($S = 20$ mm) point to plane gap in nitrogen at 26.7 kPa and the gap voltage of 4 kV. E is the intensity of electrical field at the axis of the probe. Taken from [56].

ions and electrons densities were limited to a cylindrical channel with fixed radius and the field was computed using the method of disks. The computed current induced by the streamer arrival to a small cathode probe presented in figure 9 are in Ref. [56] compared with that measured experimentally.

As typical for the 1.5D models, the claimed good matching of the magnitudes of the computed and measured experimental current waveform was apparently achieved by somewhat arbitrary choice of the constant discharge channel radius. However, the overall physical picture and the computed temporal development of the discharge current can be more critically affected by the simplistic treatment of the unrealistic high energy of electrons near the cathode surface resulting from the modified local field approximation used. Without such treatment an excessive ionization is generated immediately at the cathode, which in turn leads to an enhancement of the field etc, and the whole simulation becomes unstable. Since the physical interpretation of the current signal induced by the streamer arrival to the cathode is central for our next considerations, the results in figure 9 and conclusions by Odrobina and Černák [56] briefly discussed below are corroborated by a more advanced 1.5D model in section 4, where the high-energy electrons are treated by a more advanced and physically sound local mean energy approximation.

The cathode probe current computed by Odrobina and Černák [56], shown in figure 9, consists of an initial sharp current spike due to the displacement current followed, some 20 ns later, by a lower current hump due to the ion arrival at the cathode. The conclusion that the initial spike is due to the displacement current is in contradiction to the generally accepted assumption by Marode in [28], but has been corroborated by very recent results by Belopotov *et al* [164]. The computed current signal is relatively insensitive to changes in the photon and positive ion secondary electron emission coefficients. The results obtained show that the intense ionization indicated by the light flash on the cathode observed at the streamer arrival are not due to an intense photoelectric ([143] on page 136, and [146]) or field electron emission [156], but rather due to a dramatic increase in the multiplication factor and a release of electrostatic energy accumulated in the streamer channel-cathode system. The current hump delayed 20 ns after the current maximum is claimed to be due the positive ion arrival to the cathode. The very similar discharge current waveform with subsequent damped oscillations was observed also by Ikuta and Kondo [52] (see figure 5(a) there). Such observed current hump seems to correspond well with the 2 ns delayed current hump seen in figure 7 measured at atmospheric pressure in a highly over-volted gap and a some 10 ns delayed current spike marked B in figure 8. Note, however, that an alternative explanation for such double peak structure presented by Eichwald *et al* [152] is that a current hump delayed some 25 ns after the current maximum observed in the repetitive discharge regime (see discussion below) is due to the development of a secondary streamer starting from the anode just after the arrival of the primary streamer.

An interesting feature of the results in figure 9 corresponding well with the results shown in figure 8 is a 15 ns delay between the maxima of the current and field strength at the cathode. Thus, if a significant field emission occurs as indicated by the Curve 1 in figure 8, according to the simulations, it is expected to take place some 10 ns after the current maximum. The detailed discussion and theoretical treatment of this issue is presented in section 4.

The discharges hitherto discussed in this section were fed by single gap voltage pulses. In such highly transient, probabilistic discharge phenomena the streamer radiation is typicall studied by streak cameras and cameras in fast-framing regimes (see figure 6) that can acquire up to 10^8 frames per second with a high spatial resolution [31]. The discharge currents are usually measured by fast digital oscilloscopes in the single pulse acquisition mode with a temporal resolution on the order of nanoseconds without the need to consider shot-to-shot reproducibility (see figures 7 and 8).

Nevertheless, it should be noted that starting from the pioneering work by Marode [28], the great majority of positive streamer phenomena were studied in the high-stable dc positive repetitive point-to-plane streamer coronas, where using averaging acquisition modes the light and current signals from millions of streamer pulses were accumulated, improving the time resolution to 0.3–0.4 ns [46]. Unfortunately, in such repetitive streamer experiments the earlier discharges significantly modify the discharge's behavior. This is because the field and the background ionization, as well as the gas composition, are affected by the previous discharges. In this respect it is interesting to note also that the current signal generated by the arrival of repetitive streamers measured by small cathode probes in air [46] is very similar in shape and just some 100% higher than the typical current pulses of air DBDs exemplified in appendix in figure A2.

3.2.2. Streamer phenomena in non-uniform fields with highly stressed cathodes—complete breakdown. The streamer phenomena in negative point-to-plane has attracted much

less attention than the above discussed 'classical' streamer coronas and breakdowns in positive point-to-plane gaps. Partly it is because the negative spark breakdown voltages are significantly higher, particularly for larger gaps [165, 166]. As a consequence, comparing to the positive breakdown phenomena, there is a lack of the time- and space-resolved measurements of the initial ionization development, which is necessary to shed light on the sequence of events leading to the negative breakdown. Nevertheless, already in 1956, Fark and Cones [167] obtained very insightful results using a 10cm wide (gap spacing $S = 100$ mm) negative rod-to-plane gap in laboratory air energized by the pulsed voltages chopped at an accurately controllable time. Analyzing their still photos of the discharge, the authors revealed the positive streamer formation in a close vicinity of the 0.8 cm curvature radius ($r = 8$ mm) spherical cathode: *'With the sphere negative, the electron avalanches formed in the region near the sphere initiate positive streamers which quickly propagate the short distance to the sphere. As the streamers approach the* (cathode) *sphere, the high positive-charge densities at their tips make already extremely high gradients near the sphere even higher, and, largely because of these exceedingly high gradients, electrons are immediately release from the sphere.*' This picture corresponds surprisingly well with the streamer phenomena observed in a short rod-to-plane gap ($S = 20$ mm, $r = 10$ mm) using an image converter camera together with an image intensifier and a photomultiplier by Akazaki and Tsuneyasu [168].

Based on these results, we can hypothesize that the negative breakdowns, as well as the breakdowns in uniform fields gaps and positive point-to-plane gaps illustrated in figures 1 are unavoidably associated with the formation of an active cathode spot at the arrival of the primary positive streamer. If this hypothesis is true, than it is reasonable to expect also a similarity between the current signal induced by the streamer arrival to a cathode probe in the positive point-to-plane gaps, as those shown in figures 7 and 8, and the initial cathode current preceding the negative breakdown. Unfortunately the above described spatiotemporal measurements of the discharge radiation were not published together with the corresponding discharge currents, and in literature there is only a limited information on such pre-breakdown currents:

Both the discharge current and discharge light emission during the negative breakdown in a short rod-plane gap ($S = 10$ mm, $r = 7.5$ mm) were measured by Isa *et al* [170], where the authors found that *'Depending on the voltage pulse magnitude a steady negative corona did or did nor exist prior to the breakdown. However, in both cases the first current pulse was very similar to that of a negative corona TP with a rise time less than 10 ns.*' Such resemblance of the pre-breakdown current pulses in a rod-to-plane gaps to the negative corona TPs (discussed in detail in the following section 5.1) was observed also by, for example, by Suzuki [165]. The measured pre-breakdown current pulses had magnitude of an order lower than the positive corona current spikes in figures 7, 8, but similar to the repetitive negative corona TPs. The transition from regular TPs to a glow

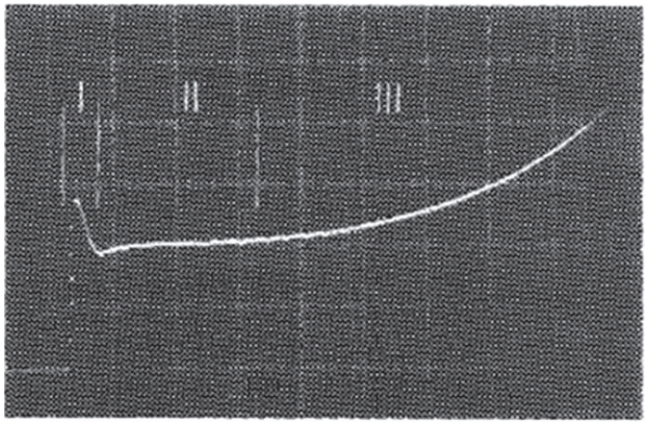

Figure 10. Oscillogram of the initial stages of a spark breakdown in atmospheric-pressure N_2 at a voltage of 6.5 kV, $r = 0.2$ mm, $S = 4$ cm (scales 2.75 mA/div and 50 μs/div), taken from Černák *et al* [169].

negative corona in a short point-to-plane gap ($r = 0.2$ mm, $S = 4$ cm) in air is clearly seen in [171, 172]. Contrary to the discharge development in air, the breakdown in short point-to-plane breakdown in electron non-attaching nitrogen is not preceded by a TP, but a fast-rising narrow current pulse shown in figure 10.

4. Streamer-cathode interaction as a bottleneck in computer simulations of the streamer breakdown

In the previous sections we summarized the sequence of events leading to the streamer breakdown and identified the streamer-to-cathode contact as a crucial bottleneck in understanding the process. Due to the complexity of the ionization processes at the streamer arrival to the cathode resulting in the formation of a glow-discharge-type cathode spot numerical simulations are very useful to provide additional insights into the physical mechanisms that are not easily studied experimentally. In this section, we present and quantify a theoretical treatment of the streamer-cathode interaction including a criticism of the simple local field approximation often used to simulate the streamer-cathode interaction and ionization phenomena in the immediate cathode vicinity.

4.1. Model

The most widely used model for simulation of streamer discharges at atmospheric pressure is based on truncated set of moments of the Boltzmann equations for charged species coupled with Poisson's equation. The truncated set of moments consists of continuity equation and momentum equations. Continuity equations for density of charges species n_α are

$$\frac{\partial n_\alpha}{\partial t} + \nabla \cdot \mathbf{\Gamma}_\alpha = G_\alpha - L_\alpha, \tag{3}$$

where G_α and L_α represent production and lost terms, and Γ_α is a flux of density n_α due to macroscopic motion of the fluid. Usually the momentum equations at atmospheric pressure can

be efficiently approximated by a drift-diffusion approximation. In this approximation, the momentum is considered to be in steady state and inertial terms are neglected. This approximation is valid when the mean free path of considered species is significantly smaller compared to characteristic spatial scale of variation of other physical quantities, e.g. n_α and the electric field $\mathbf{E}$. Note that for electrons the mean free path at atmospheric pressure is of order 10^{-7} m, while spatial scale of variation of the electric field in the head of the ionization wave is in order of 10^{-5} m. Drift and diffusion components of the momentum equations are then balanced by collisions and the flux is given by

$$\mathbf{\Gamma}_\alpha = \frac{q_\alpha}{|q_\alpha|} n_\alpha \mu_\alpha \mathbf{E} - \nabla(D_\alpha n_\alpha), \tag{4}$$

where n_α, μ_α, D_α and q_α are density, mobility, diffusion coefficient, and charge of a specie α, respectively.

Moreover it is usually assumed that energy gain by charged particles from the electric field is locally balanced by the losses due to collisions with neutrals. Note that collision frequency of electrons with neutrals at atmospheric pressure is in order of $\nu_{en} = 10^{13}$ Hz and electron energy distribution function then relaxes to equilibrium with local electric field at timescale ν_{en}^{-1}. The energy equation can be then replaced by *local field approximation*. Note that local field approximation is well justified for description of electrons in streamers that are propagating in volume, as has been show by comparison to particle in cell/Monte Carlo (PIC/MCC) simulation in [173]. Transport parameters in (4) and reaction rates in gain and lost terms in (3) then become a function of reduced electric field $|\mathbf{E}|/N_{gas}$.

In cases when local field approximation is not sufficient, it is useful to add energy transport for electrons, leading to *local mean energy approximation*. Energy equation can again be obtained from electron Boltzmann equations [174] and can be transformed to a form similar to (3):

$$\frac{\partial n_\varepsilon}{\partial t} + \nabla \cdot \mathbf{\Gamma}_\varepsilon + \mathbf{\Gamma} \cdot \mathbf{E} = G_\varepsilon - L_\varepsilon, \tag{5}$$

where n_ε is energy density, where G_ε and L_ε represent energy production and lost terms due to collisions. The term $\mathbf{\Gamma} \cdot \mathbf{E}$ represents heating of electrons by the electric field, and on the right-hand side is total energy transport by collisions. Energy flux Γ_ε can be expressed as well in drift diffusion form [174]:

$$\mathbf{\Gamma}_\varepsilon = n_\varepsilon \mu_\varepsilon \mathbf{E} - \nabla(D_\varepsilon n_\varepsilon), \tag{6}$$

where μ_ε and D_ε are energy mobility and energy diffusion coefficient. This formulation of energy equation is convenient since it can be solved by the same numerical tools as the continuity equation for charged species, e.g. [175]. Semi-implicit time discretization is of great advantage because they allow to avoid numerical instabilities and allows for much larger timesteps compared to explicit methods [176]. Transport parameters for electrons and reaction rates for electron impact processes can be straightforwardly obtained from corresponding cross sections sets using BOLSIG+ [174], both for local field and local mean energy approximation.

Transport equations (3)–(6) must be coupled to Poisson's equation. Note that Poisson's equation is used on a basis of electrostatic approximation: assuming the absence of external magnetic fields and only small current densities so that self-consistent magnetic field can be neglected. The Poisson's equation reads

$$\nabla \cdot (\varepsilon_0 \nabla \varphi) = -\sum_\alpha q_\alpha n_\alpha, \qquad \mathbf{E} = -\nabla \varphi, \tag{7}$$

where φ is the electric potential and ε_0 is the permittivity of free space.

Electrode surfaces can also emit secondary electrons under ion bombardment. Electron flux emitted from the surface $\mathbf{\Gamma}_{se}$ is assumed to be proportional the flux of impinging ions

$$\mathbf{\Gamma}_{se} \cdot \mathbf{n}_s = -\gamma_{se} \sum_{i \in \{ions\}} \mathbf{\Gamma}_i \cdot \mathbf{n}_s, \tag{8}$$

with secondary emission coefficient γ_{se}. Note that value of γ_{se} is poorly known, typical range of γ_{se} is $\in[0.001, 0.1]$. Where higher values of γ_{se} can be used to roughly account for other electron emission processes such as the impact of excited species and the field emission. An alternative approach for generation of secondary electrons is to consider Auger neutralization process [90, 177].

Another important physical mechanism that is responsible for generation of secondary electrons is photoemission. The flux of photo electrons is given by

$$\mathbf{\Gamma}_{pe} \cdot \mathbf{n}_s = -\gamma_{pe}\, \boldsymbol{\varphi} \cdot \mathbf{n}_s, \tag{9}$$

where γ_{pe} is a coefficient for photoemission and $\boldsymbol{\varphi}$ is photon flux at the dielectric surface. The photon flux at point of observation $\mathbf{r}$ due to the source point at $\mathbf{r}'$ is

$$\boldsymbol{\varphi}(\mathbf{r}) = \frac{1}{4\pi} \int_{V'} \frac{I(\mathbf{r}')(\mathbf{r} - \mathbf{r}')}{|\mathbf{r} - \mathbf{r}'|^3} \exp(-\mu|\mathbf{r} - \mathbf{r}'|) \mathrm{d}V', \tag{10}$$

where $I(\mathbf{r}')$ is the production rate of photons and is often assumed to be equal to the ionization production rate [178, 179], and μ is photon absorption that can be usually neglected [56], then the only coefficient needed to model the photoemission source term is γ_{pe} [180].

Higher moment fluids models are also formulated [181, 182]. Another alternative is an hybrid approach, coupling a particle model for a streamer head region with a fluid model for a plasma channel [183], or beam-bulk model where the bulk electrons are treated with a fluid approximation, while an electron Monte Carlo simulation is used to treat energetic secondary electrons in a fully kinetic way [90, 184–186]. For comparison of outcomes of models with varying complexity, see [187]. Alternative approaches to account for non-local corrections in the ionization source terms are also formulated and used, e.g. [56, 188–191].

Fluid models, even in simple local field approximation, can provide a fairly good description for streamer propagations in volume [187]. While for description of streamer contact with cathode, local field approximation will necessarily fail for simple reason: the closer the streamer comes to the cathode, the higher is the electric field resulting to higher ionization rate and higher electron density. There is no

physical mechanism in the model with local field approximation to stop this growth. This leads to unphysical results and collapse of the cathode sheath. The reason why the local mean electron energy approximation can eventualy work is as follows: as the streamer is coming closer to the cathode surface a strong gradient of the electron density is created. The strong gradient in density result in a strong diffusion flux of electrons *against* the electric force, thus electrons are loosing their energy, being unable to produce strong ionization. Local field approximation lacks this effect of slowing down or accelerating of electrons in electric fields, while this effect is included in the local mean energy approximation, through the $\mathbf{\Gamma} \cdot \mathbf{E}$ term in equation (5). This is because $\mathbf{\Gamma}$ contains both, the drift in the electric field and the diffusion of electrons, see equation (4).

But even higher moment approximations, may be insufficient, and obtained results must be therefore treated with highest caution, because very high electric field can be produced in the cathode sheath and transport parameters and reaction rates calculated based on two term approximation of the Boltzmann equation [192] may be incorrect since the known validity limit up to 1500 Td for the two term approximation of the Boltzmann equation solution [191, 192]. Secondly, the possibly very sharp variations of plasma parameters within the cathode sheath, with characteristic space scale down to 10^{-6} m, may become comparable with the mean free path of electrons, and there fluid approximation becomes simply inappropriate. Moreover, the appearance of runaway electrons at high values of the electric field can be expected [193].

4.2. Case study

We have implemented a local mean energy approximation model in order to reveal the spatial scales that we need to deal with during the streamer–cathode interaction. Conditions considered in these simulations are similar to those in [56] illustrated by the results in figure 9. Here, we use nitrogen at a pressure of 26.7 kPa, point-to-plain electrode geometry with a gap of 1 cm, and anode point radius of 0.2 mm, applied voltage of 4 kV. The streamer is simulated using a 1.5D model [194–199], the discharge is considered as a cylinder with a finite radius of 0.6 mm, and uniform radial distribution of charges and the evolution of the charged particle densities is solved in one spatial dimension along the direction of the streamer propagation. It is important to note that the 1.5D model captures the main characteristics of streamer propagation. With a 1.5D model, the electric field is found by slicing the plasma cylinder net charge density into discs. Using a 3D analytical formulation for the axial electric field from a disc, the space charge electric field in the electrode gap is calculated by integrating the individual contributions of the disks and their image charges in the electrodes. Similarly to [56], the discharge propagation is initialized by low electron flux from the cathode, that produces background ionization at level of $4.5 \times 10^{12}\,\mathrm{m}^{-3}$. Transport parameters and ionization rates used in this simulation has been calculated using BOLSIG+ [174], with Biagi's database of cross sections [200, 201]. Note that resulting ionization coefficient is substantially higher than that used in [56]. In the following we have used $\gamma_{se} = 10^{-2}$ and $\gamma_{pe} = 0$.

Considering that effective cross section of N_2 molecule is about $3 \times 10^{-20}\,\mathrm{m}^2$, then for neutral gas density $6.1158 \times 10^{24}\,\mathrm{m}^{-3}$, used in this simulation, the mean free path is about $\lambda_{mfp} = 5.45\,\mu$m. We define a characteristic spatial scale of electron density variation in the streamer head as

$$\Lambda_{ch}^{-1} = \frac{1}{n_e}\frac{dn_e}{dx}, \tag{11}$$

then obvious requirement for validity of the drift-diffusion approximation is

$$\Lambda_{ch} \gg \lambda_{mfp}. \tag{12}$$

Figure 11 shows electron density n_e, positive ion density n_i, electric field amplitude E and mean electron energy ε in the vicinity of the cathode (placed at $x = 0$). Left panel of figure 11 shows simulation results at time 38.4 ns, when the streamer head is 1 mm away from the cathode. Right panel of figure 11 shows simulation results at time 39.8 ns. At this moment the maximum of the electric field is no longer in the volume but at the cathode. We also see a much steeper front of the electron density at the rising edge of the ionization wave.

Figure 12 shows current and electric field at the cathode surface, E_c, during streamer–cathode interaction. Total current I_{tot} as to be measured on a cathode current probe consists of displacement current I_d and conductive current. High current peak at around 39 ns is fully attributed to the displacement current.

Figure 13 shows characteristic spatial scale of electron density variation on the edge of the ionization front Λ_{ch} and corresponding electric field in the streamer head. Condition (12) is well satisfied when the streamer still propagates in the volume, on the contrary, when the streamer approaches the cathode (moment associated with the current peak at around 39 ns) this condition is clearly not fulfilled. At the same time, the electric field rises above critical limit $E_{lim} = 1500$ Td for validity of transport coefficients and source parameters used in the model, calculated based on the two term approximation for solution of Boltzmann equation.

This clearly shows that while the drift diffusion approximation may be very well valid for studies of streamer propagation in volumes, for streamer interaction with a cathode the outcomes of the model must be regarded with highest caution, because conditions for validity of the model may be even strongly violated. Any interpretation of such results should be accompanied with strong discussion regarding validity and limits of the model.

5. Positive-streamer-like phenomena

In this section we will present a hypothesis congruent with our experiences that some phenomena of significant practical importance as TPs in negative corona discharges and the cathode-sheath instabilities affecting the high-pressure glow-

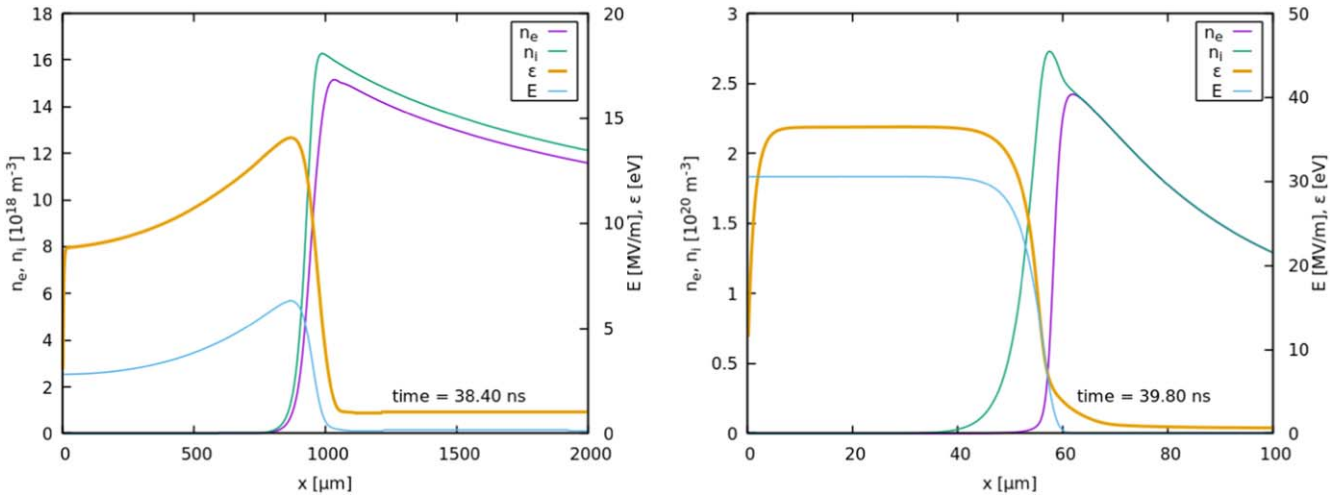

Figure 11. Electron density n_e, positive ion density n_i, electric field amplitude E and mean electron energy ε in the vicinity of the cathode at times, (left) 38.4 ns, and (right) 39.8 ns. N_2 at 26.7 kPa, Gap: 10.0 mm, $U_a = 4$ kV, streamer radius: 0.6 mm.

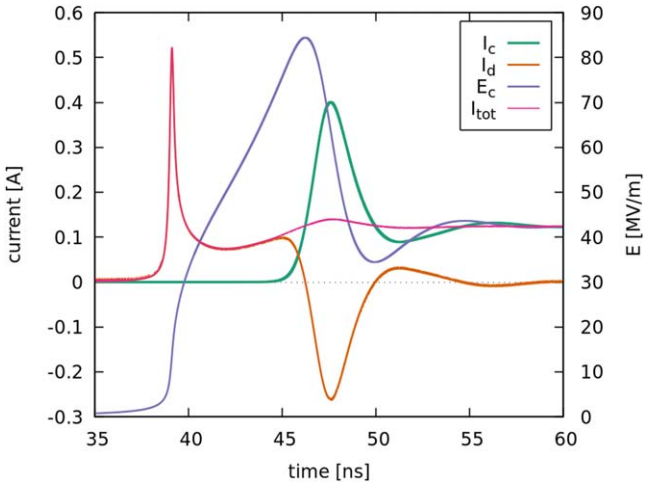

Figure 12. Current and electric field on the cathode surface during streamer–cathode interaction. I_{tot}: total current, I_c: conductive current, I_d: displacement current, and E_c electric field on the cathode surface.

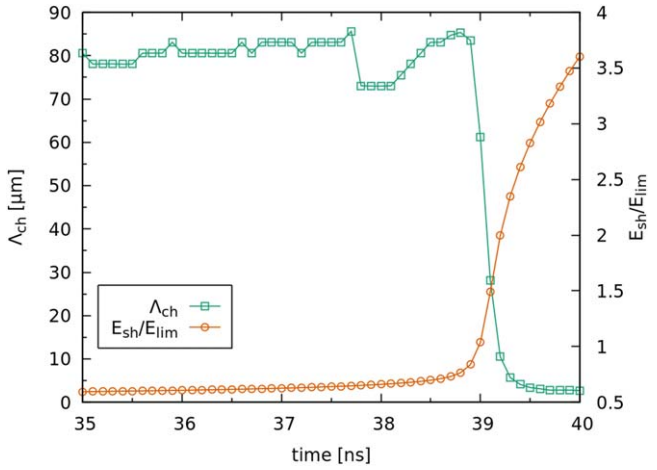

Figure 13. Temporal evolution of the characteristic spatial scale for electron density variation in the streamer head, Λ_{ch}, and the streamer head electric field E_{sh}, when the streamer approaches the cathode. $E_{lim} = 1500$ Td is the limiting reduced electric field for validity of two term approximation of the Boltzmann equation solution. Critical value of Λ_{ch} is 5.5 μm, which corresponds to mean free path of an electron.

to-arc transitions can be interpreted in terms of the positive streamer formation in the immediate ($\sim$0.1 mm) cathode vicinity and even quantitatively explained by the above presented computer simulation model.

5.1. Negative corona TPs

It is well-documented that low-current initial stages of breakdown in a short negative point-to-plane gap in nitrogen [169, 202, 203] as shown in figure 10, and in other electron non-attaching gases [204, 205] at pressures above the order of 10 kPa are discerned by a current peak marked as a stage I in figure 10, where in several nanoseconds the discharge current rises to a maximum of some 1–100 mA. Beyond the initial peak (I), the discharge current is decreasing to a glow discharge stage (II) followed by the rise to a spark (III). The initial current peak formation is illustrated by figure 14 where the initial discharge stage of the breakdown in nitrogen (1) is compared with the first corona TP in air (2) for $r = 0.2$ mm, $S = 4$ cm. The current spike in air is some 30% higher than that in nitrogen, in a correspondence with the higher values of α in air. The peaked current is associated with the formation of an abnormal glow-discharge-type cathode spot [206]. The pulse amplitude increases with α, but is relatively insensitive to the electron attachment coefficient.

From figure 14 it is evident that the discharge in air is within some 160 ns choked off by a negative space charge formed due to electron attachment. A new discharge will start again when the negative ions dissipate toward the anode in a sufficient extent [207]. In this way, regularly pulsed discharges are generated resulting in the so-called negative corona Trichel current pulses with amplitudes in the milliamps range, such as shown in figure 15, and frequencies extending to the megahertz range [166]. Note that the first TP of the pulse train such as that in figure 14, developing in a

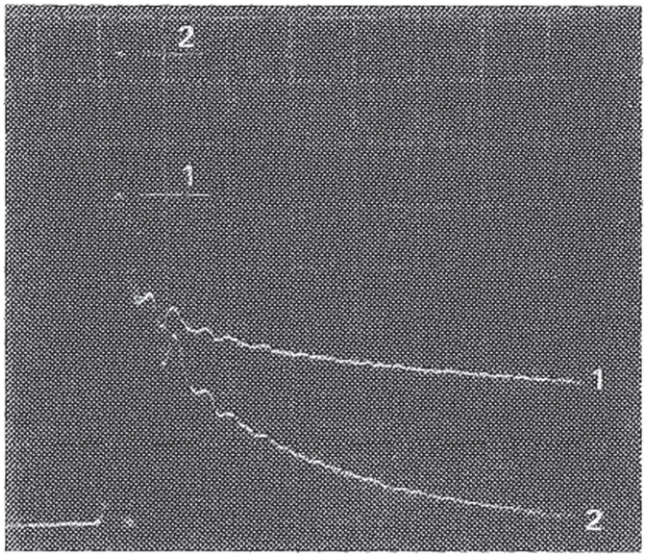

Figure 14. Oscillograms of the initial stage of a spark breakdown in N_2 (1) and the first Trichel pulse in dry air measured at atmospheric pressure air at a voltage of 12 kV, $r = 0.2$ mm, $S = 4$ cm (scales 8 mA/div and 20 ns/div, taken from Černák *et al* [169].

negative ions free space, is always larger than the subsequent regular pulses shown in figure 15.

It is an interesting and well-documented fact that the regular TPs can be generated only using cathodes with some surface imperfection as oxide spots or dust particles providing a random field (Malter) electron emission [143, 208, 209].

Since their first observation in 1938 (see the original article of Trichel, [211]) TPs have attracted a lot of attention among the researchers and engineers working in the field of applied electrostatics [212]. Quite surprisingly, despite its practical importance and the plethora of studies, the mechanism of TPs in air is still one of the most controversial issues in the physics of high pressure gas discharges.

A major source of controversy around the TP mechanism, which has been well documented but often ignored, is the very short rise time of TPs in ambient air (~1.5 ns, see figure 15) defined as the time interval in which the pulse rises from 10% to 90% of its amplitude. Apparently, it is because the measurements of TP waveforms and the understanding of their physical mechanism have always depended heavily on the availability of fast oscilloscopes with a sub-nanosecond time resolution and even more on experimental skills required for such fast TP current measurements:

The first systematic measurements of the regular TP waveforms with a sub-nanosecond temporal resolution were published in 1969 by Zentner in his excellent thesis [213] and in the subsequent papers [171, 172]. Zentner used a sampling oscilloscope with 0.35 ns rise time and found that the measured TP rise time of 1.6 ns in atmospheric pressure air is constant for the cathode curvature radii ranging from 15 μm to 5 mm [171]. It should be noted that already forty years ago Goldman and Goldman [214] stated that this quite surprising but well documented fact can serve as a critical test for models explaining the TP formation.

In papers by Zentner [171, 172], as well as in many other works discussed below it was clearly demonstrated that to follow the fast TPs current rise both the measuring resistance in series with the discharge gap and the parasitic capacitance have to be reduced to a values giving the nanosecond, or even sub-nanosecond, time constant of the measuring circuit required to follow the fast TPs current rise. In 1973, Torsethaugen and Sigmond [215] used a sampling oscilloscope with a rise time of 0.3 ns, and measured the rise times shorter than 3 ns for sharp ($r = 0.074$ mm) Mo and Au cathodes. In 1985 Gravendeel and Van der Laan published [216] the measured rise time of 1.3 ns for $r = 0.0125$ mm, lately reduced to 1.15 ns [217] by considering the measuring system influence. Their measurements were made by the measuring system with the well verified time resolution of 0.7 ns. The fact that TP rise time in ambient air is smaller than a few nanoseconds at atmospheric pressures has been confirmed by many other authors [47, 203, 210, 218–221].

Nevertheless, it is necessary to note that in the last four decades, starting by work Thanh [222] there is outburst of the experimental and theoretical works devoted to TPs in atmospheric pressure air with the measured and computed rise times on the order of 10 ns, which neither refer to the above presented results, nor consider their physical and practical implications. We can exemplify it by several recent papers [223, 224], where the measuring resistors used and the stray capacitances were far to large to measure the 1–2 ns rise time of TPs in atmospheric-pressure air. In fact we are not aware of any published results, where the 'slow-rising' TPs in air at atmospheric or near-atmospheric pressures were measured using a measuring system with a properly tested for at least nanosecond time resolution. Thus, we dare to claim that such long TP rise times were not determined primarily by the physical processes in the discharge itself, but by the improper measuring circuits used. Therefore, also numerous computer simulation models based on such disputable measurements are not realistic in explaining the TP ionization mechanism. Such models are in line with the obsolete physical picture proposed a half of century ago by Loeb in his excellent and still indispensable monograph [143], which is still widely accepted by community of engineers and applied physics researchers in the field of high voltage and applied electrostatics. For example, as supposed by Hogg *et al* '*Negative corona discharges in air initiate and sustain in accordance with the Townsend primary electron avalanches emanating from the tip of the cathode into the ionization zone. Much slower positive ions traveling in the opposite direction develop a cathode sheath which increases the field in close proximity to the sharp cathode.*' [12]. Unfortunately, as mentioned in [220] and discussed in details at the end of this section, such oversimplified physical picture can provide misleading implications for important industrial applications of TP coronas.

Beside their very short rise times, another surprising property of the TPs is insensivity of the TP waveforms to the cathode material [143, 220, 225, 226] observed particularly for sharp cathodes with, say, $r < 0.1$ mm. As a consequence, contrary to the above discussed models already in 1953 it was

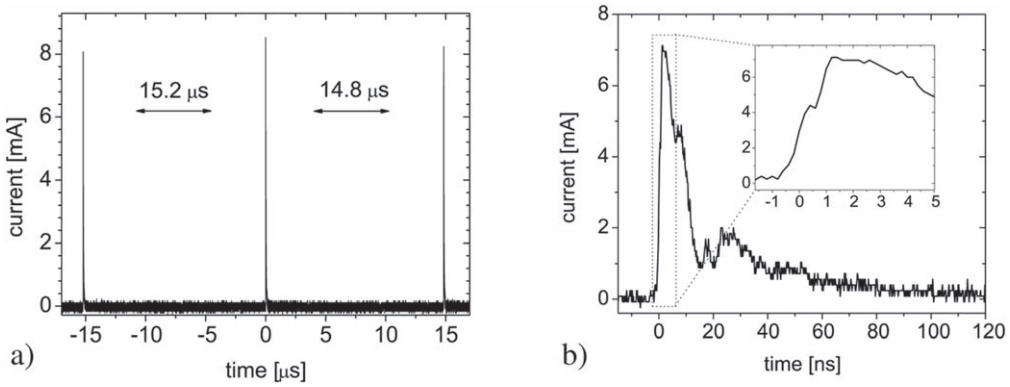

Figure 15. TPs current train (a) and the single current pulse (b) in atmospheric-pressure synthetic air using steel cathode with $r = 240$ μm, $S = 7$ mm, and voltage 6.8 kV. Taken from Hoder *et al* [210].

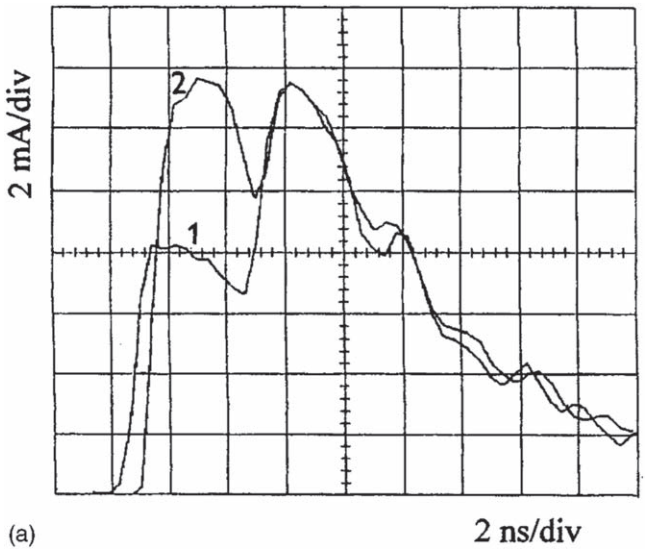

Figure 16. First Trichel pulses measured in dry air at 40 kPa, $r = 0.625$ mm, $S = 10$ mm and a gap voltage of 5.28 kV using the brass (1) and the CuI-coated cathode (2). From Černák *et al* [220].

speculated by Meek and Craggs [227] that '*A Townsend γ-mechanism may not be responsible by itself because of the corona's insensivity to cathode metal.*' In 1976 Ikuta and Kondo [228] based on their fast (~3 ns) spectroscopic study in air at a pressure of 50 Torr advanced the hypothesis that *'the development of (TP) cathode glow may be considered as streamerlike, through the secondary effect from cathode may also be active'*. In context with the results discussed in section 3.2.1 it is interesting to refer here to the results [158, 229] illustrating a striking similarity between TP currents and the current signal induced by the positive streamer arrival in a positive point-to-plane gap in air. Many arguments in favor of the hypothesis that, fast TP current rise is generated by the arrival of a positive streamer formed in the immediate vicinity of cathode to its surface can be found also in extensive studies of current waveforms of the first TPs by Černák *et al* [220, 230–232].

The results of these studies are exemplified by figure 16 illustrating the effect of the changing cathode secondary emission on stepped waveform of first TPs well discernible in air at a reduced pressure of 40 kPa using a relatively blunt cathodes [220]. The secondary emission of the brass cathode was increased by a copper iodide coating that is known to have exceptionally high photoelectric yield. The CuI coating resulted in a significant enhancement of a streamer-initiating Townsend discharge. It, however, in agreement with the computer simulation results in section 4 (see also figure 6 in [56]) had no effect on the following TP current pulse maximum generated at the streamer arrival to the cathode.

Comparing to the measurements of TPs current waveforms in atmospheric pressure air, the related optical investigations of TPs have been even more hindered by the speed and sensitivity required of the diagnostic apparatus in order to confirm the hypothetical formation of the positive streamer in the sharp cathode vicinity [47, 217, 233]. For sake of brevity, we shall restrict ourselves to a brief discussion of recent studies made using the time-correlated single photon counting method [47, 210, 233] with tens of picoseconds temporal and tens of micrometers spatial resolution used to study the regular TPs in atmospheric pressure air:

Townsend discharge generating the streamer initiating plasma, and the subsequent cathode and anode- directed streamers are shown in figure 17 (see also similar results presented by Akazaki *et al* in [168]). The measured radiation of the first negative system and the second positive system intensities [47, 210] correspond well with typical positive streamer radiation (see, for example [48, 234, 235]) in air.

Thus, the results by Hoder *et al* [47, 210] provide strong experimental evidence that the ionization phenomena resulting in the very short (~1.3 ns) rise time and the subsequent initial current decay (in some 10–20 ns) of the regular TPs in air seen in figures 15 and 17 are due to the formation of a positive streamer in the immediate (~0.1 mm) vicinity of the cathode and its arrival to the cathode such as simulated in figure 9 and in section 4. In agreement with the results of Sigmond in [206], Hoder *et al* [47, 210] observed that the streamer ignition was preceded by the formation of streamer initiating plasma during a Townsend discharge phase. This sequence of events resembles closely the pre-breakdown phenomena in positive point-to-plane gaps discussed in section 3.2.1 and illustrated by figure 1(c). Note that the spatial and temporal development of the discharge radiation

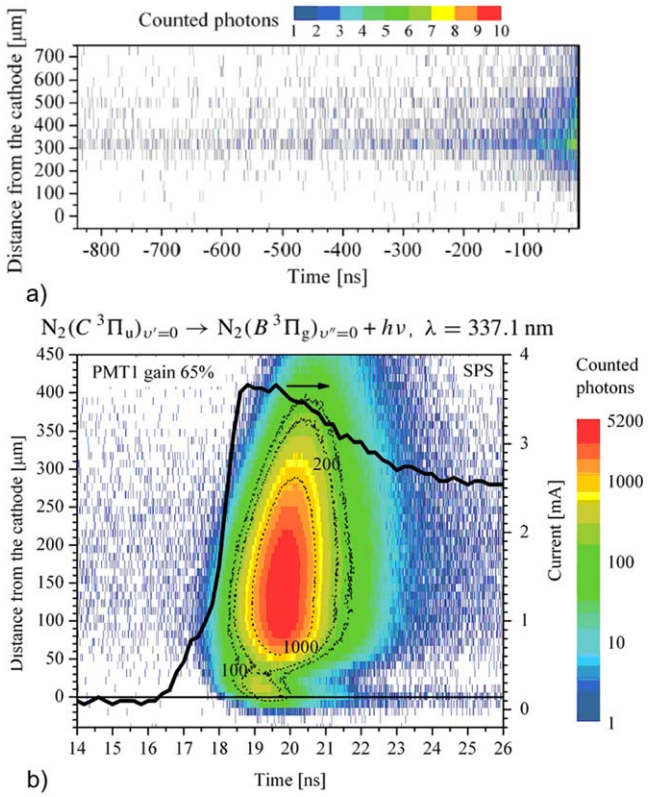

Figure 17. The measured intensity of the second positive system of molecular nitrogen using the time-correlated single photon counting technique. In the panel (a), the phase prior the Trichel pulse is shown. Slow increase of the emission intensity is visible. In the panel (b), the light emission during the actual discharge is shown. The corona discharge setup consisted of a grounded cathode with a streamers tip curvature of 190 μm and a positive dc voltage (+7.8 kV) connected plate, both made of stainless steel with a gap of 7 mm. Taken from Hoder *et al* [47].

in figure 17 reminds closely the positive streamer development in the close cathode vicinity (approx. 0.15mm) observed very recently by Hoder *et al* [235] and Nemschokmichal *et al* [71] in a pre-ionized DBD in atmospheric-pressure N_2 + 0.1 vol% O_2 gas mixture (see figure 3 in [71]). Also the sequence of events in figure 17(a), namely a slowly developing multi-avalanche Townsend discharge (approx. 1 μs, see figure 17(a)) resulting in a critical space charge accumulation and the subsequent positive streamer ignition resembles the successive avalanches of 'generation mechanism' during the pre-breakdown phenomena in low-over-voltage uniform field illustrated in figure 1(a) and the formation of a streamer initiating plasma ('initiating cloud') by many 'sub-critical' avalanches in positive point-to-plane gaps discussed in section 3.1.2.

The occurrence of a cathode-directed ionizing wave during the TP rise, resembling that observed by Ikuta and Kondo [234] at a pressure of 50 Torr and the results in figure 17, has been indicated by several computer simulation models [221, 236–239]. These simulation models are, however, complicated by limitations of the local field approximation in the cathode vicinity moreover augmented by the strongly non-uniform Laplacian field. As a consequence (see section 4), many very basic properties of TPs are inaccessible in these simulations. For example, contrary to the experimental facts, the computer simulation results are in general [197] very sensitive to the assumed type and efficiency of secondary electron emission from the cathode.

The results by Hoder *et al* [47, 210] taken together with the observed [158, 229] similarities between the current signal induced at the streamer arrival to the cathode in a short point-to-plane gaps and TP waveforms (see also figure 20 in the next section) invite a not unreasonable assumption that the basic properties of typical TPs in air, particularly the fast 1.5 ns current rise and the subsequent initial (~10 ns) decay, can be understood in terms of the simulation model presented in section 4. Such a hypothesis enables one to explain [220] the fast ionizing phenomena resulting in the short rise time of TPs in the terms very similar to the positive point-to-plane streamer phenomena discussed in sections 3.2.1 and 4: after, dE_c/dt (and the positive streamer velocity) simultaneously passes its maximum (see figure 12), the displacement current stop to rise, and subsequently decreases rapidly as a result of a reduction of electron multiplication path and saturation of the α-coefficient. As indicated by the experimental results of Černák *et al* [220] in the case of TPs the streamer arrival is preceded by a Townsend discharge feedback by cathode photoemission. This provides also a plausible explanation for stepped forms of TPs observed particularly at reduced pressures and using blunt cathodes [172, 225, 230, 231, 240] exemplified by figure 16. For TPs from sharp cathodes with small surface areas in atmospheric-pressure air such Townsend ionization apparently manifests itself just as a short step on the TP leading edge seen in figures 15(b) and 17(b).

As mentioned in the Introduction, our review is not aimed to discuss the applications of streamer discharges. However, at the end of this section it is useful to explain how the recent theoretical models of 'slow-rising' TPs [224, 241–243] based on apparently incorrect experimental data [223, 224] can mislead the workers in the field of applied electrostatics.

The simulation models in [243–246] (and similar others) are based on the measurements of TPs current waveforms made using measuring resistors 1 and 2 kΩ.

Even when the corresponding parasitic capacitances were not mentioned, the measuring resistors used are evidently far too large to measure the 1.5 ns rise time of a TP. As a consequence, the measured long TPs rise times shown in the figure 18, which disagree strongly with the results by Zentner (see reference [171]) are not determined by the physical processes in the discharge itself. In fact, the results figure 18 are due to the measuring circuit (integration) response to the TP waveforms with the nearly constant ~1.5 ns rise times with magnitudes increasing with cathode radii [171, 172].

The all criticized computer simulation models of TPs [242, 244, 245] based on the data like those in figure 18 (or in [247]) assume that the TP current growth is in a short time, which roughly equals to the TP rise time, choked off mainly by a negative ion space charge formation, as explicitly stated in [248]: *'The impact of the ionization and attachment coefficients on the rise time of the pulses could be studied in the*

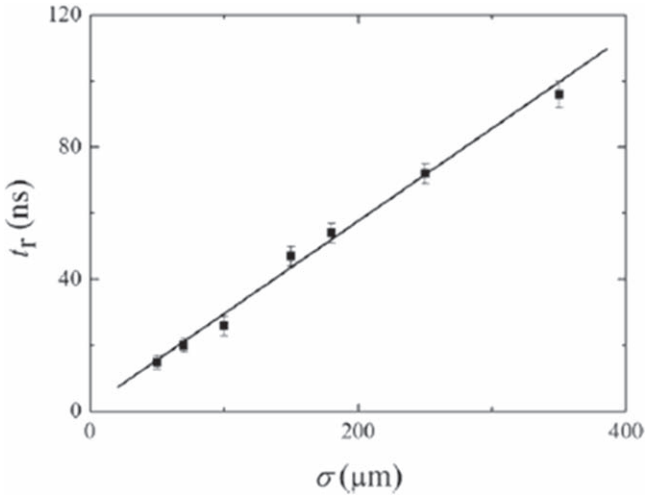

Figure 18. Rise times t_r of the regular TPs in ambient air for different cathode radii σ measured using a slow-response measuring circuit. Taken from [245].

light of the role the avalanche ionization plays in forming the rising side of the pulse. The higher rate of the avalanche ionization process, the sharper the rising side of the pulse. Since increasing the attachment coefficient enhances the rate of dissipation of electrons, it will decrease the rate of the avalanche ionization and hence, lengthen the rise time of the pulse.' However, the proposed role of the electron attachment is in contradiction to the results shown in figures 10, 14. Moreover, it assumes (particularly if not some 10–50 ns rise times as in figure 18, but the real TP rise time of 1.5 ns is considered), a very fast electron attachment in the cathode ionization region, i.e. in less than some 0.4 mm according to figure 17 and some 0.2–3 mm from the cathode surface according to the simulation results in [241, 246].

A consequence of the fast electron attachment in the cathode immediate vicinity assumed in the models ([242, 244, 245] and many others) is that the rest of inter-electrode space is supposed to be filled solely with negative ions. On the other hand, there is a strong experimental evidence for a significant density of free electrons in electrostatic precipitators and other practical devices based on the negative corona charging process several cm away from the cathode [249–251]. Such free electrons can be efficient particularly in charging nanoparticles [252, 253]. Thus the criticized models [242, 244, 245] call away from considering the free electron charging in electrostatic precipitators, which can results in their poor construct and improper design.

5.2. Cathode-sheath instabilities in high-pressure discharges

Except for the so-called Penning gas mixtures characterized by a high gas ionization at relatively low electric field hindering the formation of rapid field gradients and large space charges [8, 254], it is generally agreed to be difficult to reliably control diffuse discharges at near-atmospheric pressures. It is because even small variations of the amplitude or repetition frequency of the applied voltage, minor changes in the electrode geometry and surface properties, in gas flow and pre-ionization, etc, can lead to discharge plasma instabilities causing a transition from the relatively unstable diffuse mode to that of a much more stable filamentary discharge.

As discussed in section 3.1.2 the gas discharge instabilities resulting in the plasma filamentation have been extensively studied to improve the performance of TEA lasers [117, 118]. More recently, these phenomena are studied in the context of large-area diffuse plasmas and micro-discharges [5, 255, 256]. There is a large body of literature in this field, nevertheless it is still surprisingly contradictory:

For example, according to the current review by Bruggeman *et al* [5] '*The most common instability is the so-called thermal instability. This instability is triggered by small fluctuations in the electron density that lead to the following chain of events. An increase in electron density leads to increased Joule heating and thereby a localized increase in the gas temperature and decrease in gas background density. ... The above description of instabilities suggests that instabilities occur in the bulk plasma and indeed contractions of the positive column of atmospheric pressure glow discharge have been observed.*' On the other hand, for example according to the review by Kunhardt [255] '*Since the largest electric field of a self-sustained discharge typically occurs in the cathode boundary region, the glow-to-arc transition is likely to be initiated by fluctuations in the field of this region.*' This assumption is supported, for example, by Akishev *et al* [257] claiming that '*Fast formation of the high-current density current spots (which are not the hot arc spots) on the electrodes strongly influences the homogeneity of the electrical breakdown of the gas gap at higher pressures and initiates the non-uniform constriction of the plasma column farther if the initial breakdown was homogeneous.*' (see also figure 4 and the related discussion in section 3.1.2). This is in accord with the already a half of century old claim by Loeb [258] that '*The circumstance that in relatively high fields the negative carriers are mobile free electrons, while the positive carriers are the more sluggish gaseous ions, leads inevitably to conditions which can make the cathode region a source of instability in many gaseous discharges. Such instabilities now appear to be much more common than heretofore suspected. They manifest themselves in peculiar phenomena whose nature and common origin have remained obscure.*', which is supported by many more recent works as that of Akishev *et al* [257].

In this section, we will attempt to discuss some of the 'peculiar phenomena' mentioned by Loeb, in terms of instabilities related to the positive streamers formed in the narrow cathode regions of high-pressure glow and Townsend discharges. We suggest that such fast positive-streamer-like phenomena associated with the cathode spots formation can be very common but hardly observable initiators of '*An increase in electron density (that) leads to increased Joule heating and thereby a localized increase in the gas temperature*' mentioned by Bruggeman *et al* in [5].

The following considerations are partly a continuation of the discussion in section 3.1.2 related to the streamer breakdown of the cathode region in conditions of TEA laser discharges and TPs in section 5.1. In this context, an interesting

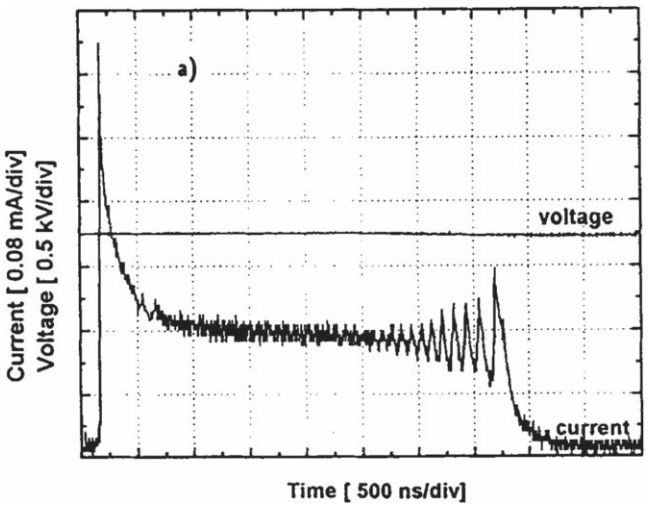

Figure 19. Oscillations on the plateau of the first Trichel pulse current in hydrogen at a pressure of 35 kPa (brass cathode of $r = 0.15$ mm, $S = 10$ mm). Taken from [261].

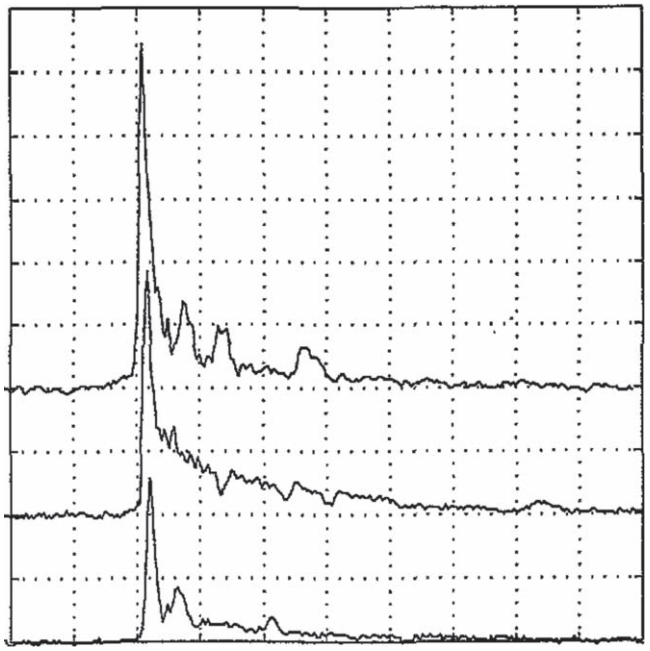

Figure 20. Peculiar current pulses observed during a glow discharge phase using the unconditioned cathode surface at the same conditions as in figure 12, but at relatively low gap voltage values. (Scales 5 mA and 50 ns per division.) Taken from Černák *et al* [150].

type of instabilities, that hitherto has attracted remarkably little attention in the literature is an ionizing wave driven cathode-sheath instability with a repetition period of 25 ns theoretically proposed by Bityurin *et al* [259, 260] for a glow discharge cathode region in N_2 at atmospheric pressure. Such proposed periodic ionizing waves can have much in common with the current oscillations with the period of some 100 ns '*reflecting the back and forth motion of the electric field in the cathode fall region*' computed by Morrow [197] at a reduced pressure of 6.67 kPa for a negative point-to-plane gap. Experimentally, similar current oscillations with a period of 20 ns were observed by Kondo and Ikuta [52] in a filamentary glow discharge formed by the streamer arrival in air positive point-to-plane gap at 100 kPa. Figure 19 illustrates the peculiar discharge current oscillations with a period of some 100 ns observed by Zahoranova *et al* [261] on a glow-discharge plateau of first TP in hydrogen at a pressure of 35 kPa.

Still not well understood effects of the conditioning of high-pressure discharge gaps by passing a number of sparks are of a significant practical interest, since the cathode conditioning has been widely used to prevent or delay the glow-to-arc transition and to affect the breakdown voltage–time characteristics [150, 262, 263] (see also figure 10). It is generally accepted that the conditioning effect, such as illustrated in figure 10, is due to the destruction of cathode emission sites as protrusion sites, oxide spots, or free particles. Nevertheless, as indicated by recent computer simulations [264], the effect of cathode surface protrusions on high-pressure discharges, where the sheath properties are critical, are still known only in the most superficial terms, even for the apparently simple steady state in argon. Unfortunately, the related phenomena inside the narrow ($\sim$10–100 μm) high-pressure cathode sheaths, which are typically random in time and place, are not amenable to optical studies with the necessary temporal and space resolution [119, 120]. However, as already discussed in section 3.1.2, some insight into the dynamics of high pressure cathode spots can be obtained from the fast discharge current measurements.

As discussed in [169] (see in figure 3 there), the imperfections of the cathode surface, at higher over-voltages in an ambient air positive point-to-plane gap results in fast ($\sim$50 ns) glow-to-arc transition following the streamer arrival to the cathode. However, at the lower over-voltages the cathode surface imperfections result in a 'peculiar current waveforms' characterized by irregular narrow fast-rising current pulses of few milliamperes magnitude riding on a glow discharge bias current shown in figure 20. Note that such irregular current pulses are discernible also in figure 7:

As illustrated by figure 21(a), at reduced pressures such fast-rising pulses can be rather regular, and as shown in figure 21(b) the similar regular pulses were observed also using unconditioned cathodes in negative corona gaps (see also figure 2 in [158], and figure 21 in [231], and here see figure 20(b). A comparison of the smooth current oscillations of the transient glow discharge currents computed for a negative point-to-plane corona by Morrow (see figure 11 in [197]) and measured in a positive point-to-plane corona in air by Kondo and Ikuta [52] with the fast-rising regular pulses from the unconditioned cathodes in figure 21 invites the following speculation: it can be hypothetized that the smooth electric field and current oscillations due to '*reflecting the back and forth motion of the electric field in the cathode fall region*' [197] can be an intrinsic phenomena for high-pressure filamentary glow discharges. However, if some cathode surface imperfections are present, they can emit a burst of electrons just at the maxima of the periodic field oscillations. The sudden electron field (Malter) emission can, similarly as

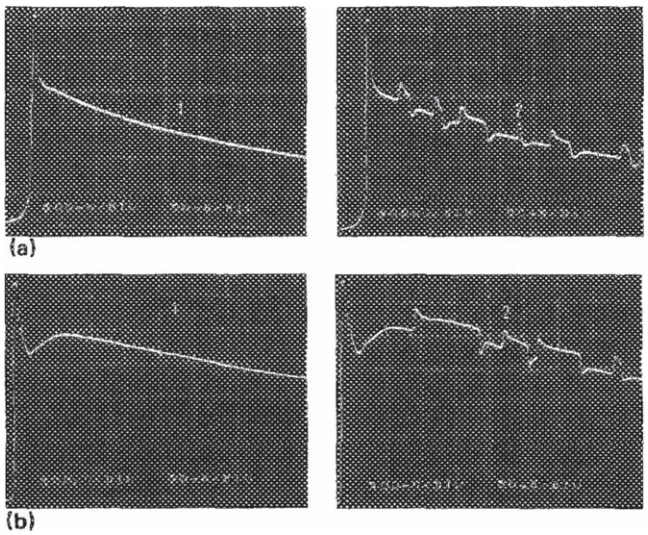

Figure 21. Comparison of (a) single positive-corona primary streamer waveforms at 3.5 kV ($r = 0.02$ mm, $S = 1$ cm) with (b) the first Trichel pulses at 6 kV corresponding to a 6/3.35% over-voltage ($r = 0.37$ mm, $S = 1$ cm) taken using the conditioned (traces 1) and the freshly polished (2) Cu cathodes. The voltages were selected to match magnitudes of pulses (a) and (b). All the waveforms were taken in dry air at 26.6 kPa. Scales: 10 mA and 50 ns per division. Taken from [158].

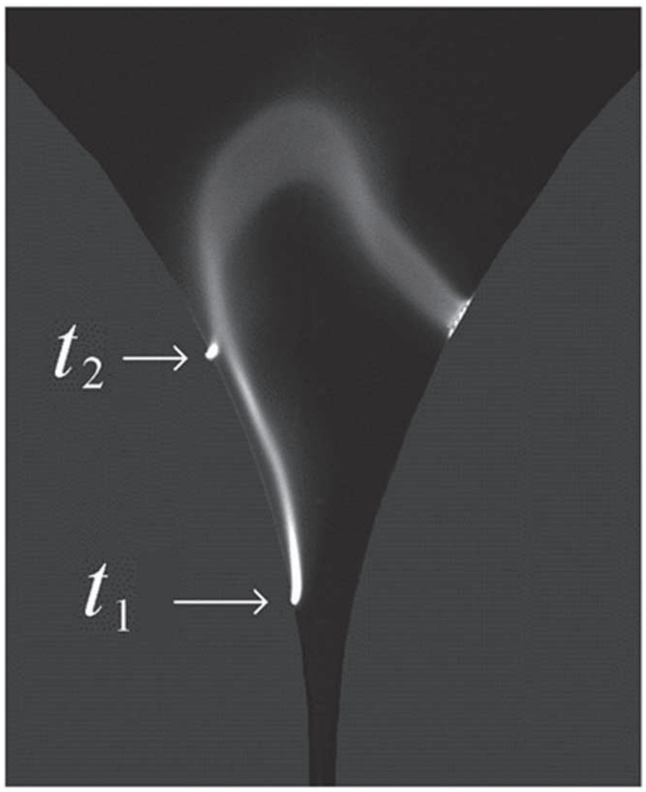

Figure 22. The formation of the new glidarc cathode spot downstream. The air flow velocity in the central part of the glidarc gap is 20 ms^{-1}. The cathode is at the left. Taken from [267].

simulated by Černák *et al* [117] and illustrated by figure 4, ignite a positive streamer-like ionizing wave in the cathode region resulting in the fast-rising and narrow current pulse characteristic (see figures 9 and 12) for the streamer arrival to cathode, such as the regular pulses seen in figure 21. Note a significant similarity in shapes of the pulses (a) and (b) (of figure 21) that corroborates the positive streamer mechanism for negative corona TPs. As documented by figure 2 in [158], at the static onset voltage such narrow 'peculiar pulses' observed using the unconditioned cathodes can be nearly identical with the first TP, and the subsequent regular TPs.

As a consequence, we can hypothesize that the regular TPs, which are currently amenable to high-sensitivity sub-nanosecond optical and current measurement (see section 5.1), and the above discussed fast-developing instabilities are of the same basic physical mechanism. If it is so, then the more detailed study of the regular TPs in electronegative gases can yield new insight into the hitherto obscure instabilities in the high-pressure cathode regions, and also into the cathode region dynamics in general. Note that the techniques developed by Akishev *et al* [265] and Mizeraczik *et al* [266] enable to generate and study repetitive negative corona current pulses also in electron-non-attaching gases and in space-charge free gaps.

In sections 3.2 and 4 a computer simulation model was proposed for the cathode spot formation which can qualitatively account also for the fast-rising current pulses of magnitudes on the order of 1–100 mA corresponding to TPs and, supposedly, also to many high-pressure discharges instabilities and micro-breakdowns phenomena. An interesting manifestation of such phenomena could be, for example, the formation of a new glidarc cathode spot shown in figure 22 associated with irregular current pulses of some 100 mA magnitudes, where '*a kind of repeated breakdown is possible between the cathode and the point on the primary positive column*' [267]. Note, that the same team of authors observed similar '*characteristic oscillatory current waveforms*' also during the glow-to-arc transition in a coaxial air plasmatron [268].

6. Conclusions and summary

This review attempts to provide a unified physical picture of ionization phenomena leading to electric gas breakdowns associated with the formation of primary streamers in short discharge gaps preferably with bare metal electrodes, the emphasis is being laid on details of the formation of active glow-discharge-type cathode spots.

Such awkward, but still not satisfactorily detailed specification is necessary to minimize misunderstandings related to the basic terms 'electric gas breakdown', 'streamer breakdown' and 'primary streamer'. As indicated by Hudson and Loeb, and briefly discussed in section 2, the need for more correct terminology regarding the breakdown phenomena emerged more than a half century ago [14]: '*Some common misunderstandings can be avoided if a careful distinction is made between the terms breakdown and spark breakdown.*' Unfortunately, in the recent literature not only the spark breakdown but many other not well defined terms as low and

high pressure breakdowns [269], pre-Townsend [270] and Townsend breakdowns [271], streamer and leader breakdowns [272], partial [273] and corona breakdowns [274], and streamer-like breakdowns [275] are used just within the relatively narrow topic of our review. Nevertheless, since in the technical literature the term 'electric breakdown' usually means the process of plasma production in an external electric field, [276], as already suggested in the Introduction, the simplest way to avoid of such complex and confusing terminology is to apply the term 'electric breakdown' as a synonym for all types self-sustained gas discharges, where the gaseous insulation breaks down and an electric current flows the gap.

For the considered unification of the ionization phenomena discussed in our paper, crucial is the exact specification of the terms 'streamer breakdown' and 'streamer breakdown mechanism'. As discussed in section 3, these terms were originally defined to characterize exclusively the fast ionization growth from a single electron avalanche to the spark in short overvolted uniform field gaps. Because of experimental constrains the related single avalanche to streamer transitions were directly observed only in cloud chambers applied to uniform field gaps at approximately $p.d > 760$ Torr cm (where d is the electrode gap, p the pressure) [277]. Observations of the transition of a single avalanche to streamer obtained exclusively in such rather special conditions were used by Raether and Meek in their well-known empirical criterion for the breakdown process termed as 'streamer breakdown'. It was not realized at that time, that the observed fast spark breakdowns can be obtained only with over-voltages above some 100% of V_s [277]. Nevertheless, later it was specified by Loeb [278] for the low-overvoltage breakdowns that '*Uniform fields at threshold and over-voltages have been convincingly analyzed by Raether's group at Hamburg. At threshold, breakdown begins as a Townsend glow discharge with secondary cathode action. Through space charge accumulation this goes over to a streamer spark*', which was subsequently affirmed by other authors [97] and theoretically explained by Hodges *et al* [20].

As indicated by figure 1 and the related discussion in section 3.1.2, Marode used the term 'streamer breakdown' strictly in the traditional way only for the breakdowns initiated by the critical single avalanche in a uniform field gap. However, as discussed in section 3.2.1 historically it has developed that his pioneering work on the streamer phenomena in short point-to-plane gaps [159] has motivated researchers to use the terms streamer breakdown and streamer breakdown mechanism for a large variety of filamentary gas discharges, where the primary streamers are initiated from a large variety of streamer-initiating plasmas. Such streamer-initiating plasmas are typically created by multi-avalanche ionization processed, such as those discussed for the uniform field gaps in sections 3.1 (see figures 1 and 4) and for the non-uniform field gaps in section 3.2 (figure 3), and section 5.1. This more general terminology, where the term streamer breakdown is used for all gas breakdowns associated with a streamer formation, is increasingly common. Unfortunately, such terminology is often used in an improper and misleading combination with the single avalanche breakdown criterion. The resulting misunderstanding is well apparent from considerations presented in the following very recent review papers:

In his first topical review Brandenburg [8] ascribed the streamer initiation to a multi-avalanche process '*At medium, normal and even higher pressures, gas discharges tend to constrict due to the streamer breakdown mechanism. Electron avalanches create a space charge and thus an additional electric field which enhances the growth of secondary electron avalanches locally. Consequently, the ionized region and the perturbation of the electric field grows rapidly and forms distinct plasma channels.*' In the second review by Bruggeman, Iza, and Brandenburg [5] the authors also mentioned such multi-avalanche streamer initiation (see figure 5 therein). Nevertheless, subsequently the authors considered only the single avalanche breakdown criterion '*While the Townsend-criterion provides the inception voltage for the Townsend mechanism, the Meek criterion (sometimes also referred to as the Raether criterion) describes the conditions for streamer initiation.* '

As briefly indicated in section 5.1 related to the TP mechanism, the unclear definition of the term 'streamer breakdown' traditionally associated with the single avalanche breakdown (see figure 1(b) should not be regarded as merely a terminology problem. This is a matter of great concern in solving many other applied problems as, for example, the long-standing problem of a general criterion for the corona onset and for spark-breakdown in non-uniform fields. As briefly discussed in section 3.2.1, this problem is apparently due to persistent unsuccessful attempts to develop new empirical and semi-empirical breakdown criteria by over-simplified modifications of the single avalanche Raether–Meek criterion [80, 274] without accepting the multi-avalanche streamer initiation.

It is hoped that the proposed specification of the terms 'streamer breakdown' and 'streamer breakdown mechanism' can define away many difficulties and misunderstandings in the theory of streamer breakdown phenomena and will make it more understandable for the applied research scientists and engineers. This paper is an attempt to step in this direction by providing a unified model generalizing the sequence of events leading to the spark breakdown for short uniform fields, positive point-to-plane and negative rod-to-plane gaps, and for streamer-like instabilities in the cathode region of high-pressure gas discharges. Based on the facts discussed in sections 2 and 5 we claim that even when the streamer breakdowns can be extremely varied and change a lot according to the experimental conditions, in general any streamer breakdown consists at least from the first three of the following most important stages:

(i) The avalanche stage, wherein the streamer initiating charge in a localized region is formed by charges generated in a single avalanche or more often accumulated in a sequence of avalanches. This stage which is often nearly imperceptible (see, for example

'successive avalanches' in figure 1(a) and transient Townsend discharge in figure 20) and at other times obvious (see, for example 'initiating cloud' in figure 6, and 'virtual plasma anodes' in close proximity of the cathode surface, see figures 6 and 22.

(ii) The positive streamer initiation: after an initial delay, when the streamer initiating charge partially shields itself from the external field forming a 'critical' region of relatively dense plasma (10^{13}–10^{15} cm^{-3}) resulting in the primary positive streamer starts to propagate.

(iii) The positive streamer propagation, where the primary streamer head propagates as a luminous spot of the diameter typically less than 1 mm with the velocity usually in the range 10^{7}–10^{8} cm s^{-1} followed by a less luminous streamer trail. As discussed in section 1 the streamer properties are rather insensitive to changes of the gas composition or the source of the seed electrons.

As assumed in section 2, the success of computer simulations in explaining the above sequences (i)–(iii) can be regarded as a measure of their theoretical understanding (see section 1). If it is true, then we can claim that these initial stages are at present fairly well understood, at least in general terms.

(iv) The streamer arrival to the cathode, forming an active glow-discharge type cathode spot, which is effectively producing the electrons by direct impact ionization in the cathode fall and, consequently, marks a turning point in the streamer-initiated formation of self sustained discharges. At atmospheric pressure the cathode spot develops in several nanoseconds and, as discussed in sections 1–5, the fast-rising displacement current peak (see figures 2, A2, 7, 8, 9, 10, 14, 15, 16, 17(b), 19–21) generated during this phase is rather independent on the gas composition, cathode secondary electron emission, and experimental conditions. As in-depth discussed in section 4, this stage has been a major bottleneck in the computer simulations of the streamer breakdowns resulting in an arc or spark formation since, as considered in agreement with our opinion in [152] (see section 4) '*It is probably a kinetic description that would be able to precisely simulate the cathode sheath formation when the streamer arrives at the cathode.*' Note that although in homogenous or weakly inhomogeneous fields the streamer arrival to the cathode is sufficient to induce the following Stage (v), in strongly inhomogeneous fields it is not a sufficient condition for the arc formation.

(v) The filamentary glow to arc transition is often characterized by the growth of secondary streamers (see, for example, figures 1, 2 and 5). Because of its significant practical importance, it has attracted a great deal of attention in the literature on both empirical and theoretical planes, but the published results on the subject are surprisingly inconsistent and, therefore are not discussed in our review. Nevertheless, based on our results discussed in sections 3.2.1 (see figure 8) and 5 we believe that a significant source of the controversy is that the existing models describing the glow-to-arc transition rely on various processes in the residual streamer channel, neglecting the processes taking place in an abnormal glow-discharge-type cathode region created by the streamer arrival including the positive streamer-like instabilities just discussed in section 5.

We believe that the theoretical model using the above specified terminology and based on the clearly defined streamer breakdown stages offers the attractive feature of the unification of a wide scale of the streamer breakdown phenomena discussed in our topical review. Moreover, it can serve as a necessary guide in the integration of our knowledge and selection of cases for further study of streamer breakdown phenomena both by experiment or computer simulation. For example, as suggested in section 6 the periodic negative corona pulses, which are good amenable to experimental study, can be used to yield a new insight into the cathode spot formation at the streamer arrival. Also, we believe that some of the discussed experimental and theoretical approaches can be applicable, for example to the streamer phenomena in RF and microwave electric fields described in [279, 280].

The purpose of the review is not to compile a catalog of references, but to give an overview of the field and its trend in line with several important topics in recent high-pressure gas discharge physics. The current rapid proliferation of applications of atmospheric pressure plasmas makes it difficult to cover both basic physics of the streamer discharges and their application in a single review article. As a consequence, the review has been preferably attempted to provide a more consistent theoretical description of the streamer breakdown phenomena. It is apparent that more experimental and theoretical research is needed to establish a well elaborated and verified theory in this field. Nevertheless, we believe that the recently developed experimental techniques and approaches [141, 281–286] or advanced computer simulation methods (e.g. to name a few [287–292]) when applied together have the potential to meet this challenge.

Acknowledgments

This research was funded by the project LO1411 (NPU I) of Ministry of Education Youth and Sports of Czech Republic and by project LM2018097 funded by the Ministry of Education, Youth and Sports of the Czech Republic.

Appendix. Implications for DBDs

Since the boundary conditions at the streamer arrival to the cathode (dielectric and metal) and the subsequent discharge development in the multitude [293, 294] of DBDs can be rather different, a detailed discussion of the streamer phenomena in DBDs is beyond the scope of this review. Nevertheless, since the early phases of breakdown in the volume DBDs burning between two parallel electrodes are similar to those without dielectric [8, 295], it might be useful to digress briefly on the controversy in the streamer initiating

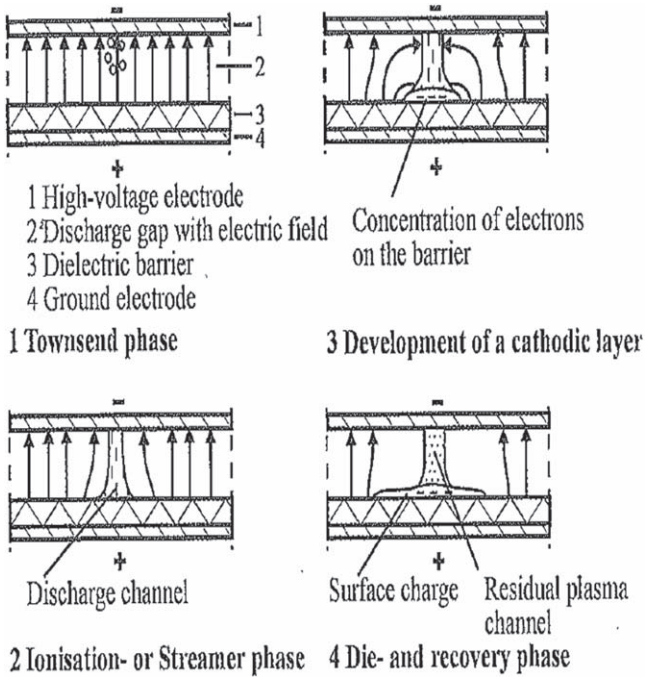

Figure A1. Schematic representations of stages of an individual DBD streamer discharge according to [127].

plasma formation in the volume DBDs in air, that is identical to the above discussed *'paradoxical situation of a streamer breakdown mechanism for spark in uniform fields.'* [107]:

For a standard DBD filamentary discharge in air, the streamer initiating plasma formation was for first time discussed in details by Kozlov [44] as the controversy between *'Electrical breakdown* via *avalanche-to-streamer transition'* mechanism as used in, for example [295–299], and *'Accumulation of positive space charge followed by the cathode-directed streamer'* mechanism that was for first time considered in 1986 by Yoshida and Tagashira [300].

Based on the experimentally observed weak but profound pre-breakdown anode glow of a microsecond duration, Kozlov suggested a more complex model based on the second mechanism, i.e. the generation of the streamer initiating plasma by a temporary Townsend discharge (i.e. a multi-avalanche charge accumulation). Kozlov's model is in agreement with the results of computer simulations by Yurgelenas and Wagner [301] and accepted in reviews by Kogelschatz and Salge [127] (see figure A1) and by Brandenburg [8].

As illustrated by figure 2 (see, for example, also Williams *et al* [29]), the current signal corresponding to the positive streamer arrival to the cathode in an uniform field gap with bare electrodes is usually obscured by a superimposed background discharge current. However, as illustrated by figure A2, in DBDs it typically takes the form of a well discernible current peak with a rise time of approximately 1ns and magnitude of some 20–200 mA [55, 297, 302]. Generally, the pulse rise times were rather insensitive to the gas composition for 0.1–10 vol% O_2 in N_2 [303], but dependent on the gas pre-ionization. Note also that the pulse magnitudes increased strongly with increasing α coefficient, and were not significantly affected by the electron attachment. The fine structure of the current pulse rising slope in DBDs is nevertheless still an unclear subject which needs experimental clarification. To resolve temporally this fast nanosecond process in detail with sufficient sensitivity, a properly designed electrical system is needed. See e.g. the discussion in [55]. It is worth noting that Höft *et al* [303–306] have recently conducted systematic investigations to inspect the influence of multiple parameters (gas composition and flow, pre-ionization, pulsed voltage steepness etc) onto the DBD micro-discharge features: current signals, streamer velocities, streamer diameter development or the spatiotemporal patterns of the light emission.

Because of the practical importance to analyze partial discharges in air-filled cavities of HV insulation systems, the most detailed investigations, concerning DBD pulse shapes have been reported for such discharges [307–309]. It is notable that for this type of DBDs the terminology is well established since the narrow current pulses with rapid rise times as that in figure A2 are unambiguously associated to streamer-like discharges and the streamer mechanism [307]. As observed by Morshuis and Kreuger (see figure 8 in [309]), at certain conditions in thin dielectric voids ($\sim$0.1 mm) the streamer current pulse can be preceded by a well-discernible slow rising Townsend discharge current.

In more complicated DBD geometries however, as for instance in the case of the surface barrier discharge, the agreement and/or the broad acceptance of the sequence of fundamental ionization phenomena leading to the well developed surface discharge is not apparent. This fact is surprising as this kind of DBD is intensively studied for multiple applied as well as fundamental research purposes [8, 310–313]. In our opinion, it is caused mainly by the asymmetry of the arrangement where one electrode is exposed to plasma while the other completely embedded into the dielectric barrier. As a result, in each polarity the mechanism of the discharge development is different (i.e. the measurable parameters differ typically in orders of magnitudes). It is complicated by effective charging of the dielectric surface by species of different mobilities (electrons, positive and negative ions). While the generation of the positive streamers in positive surface electrode polarity is understood, the negative polarity remains experimentally unverified. For negative surface electrode the issue resembles that one as in the case of metal electrodes discussed for TPs and cathode-sheath instabilities earlier in the text. The behavior is similar (yet not identical!) to the negative corona discharge in the Trichel pulsed mode. The generation of a well localized microscopic plasma on the dielectric surface in front of the cathode followed by microscopic positive streamer propagation towards the cathode (which is crucial for further discharge development) was theoretically proposed in [311]. Nevertheless, this significant discharge phase is still not well validated by experiment [314]. Typically the photoemission from surfaces is assumed to play a major role.

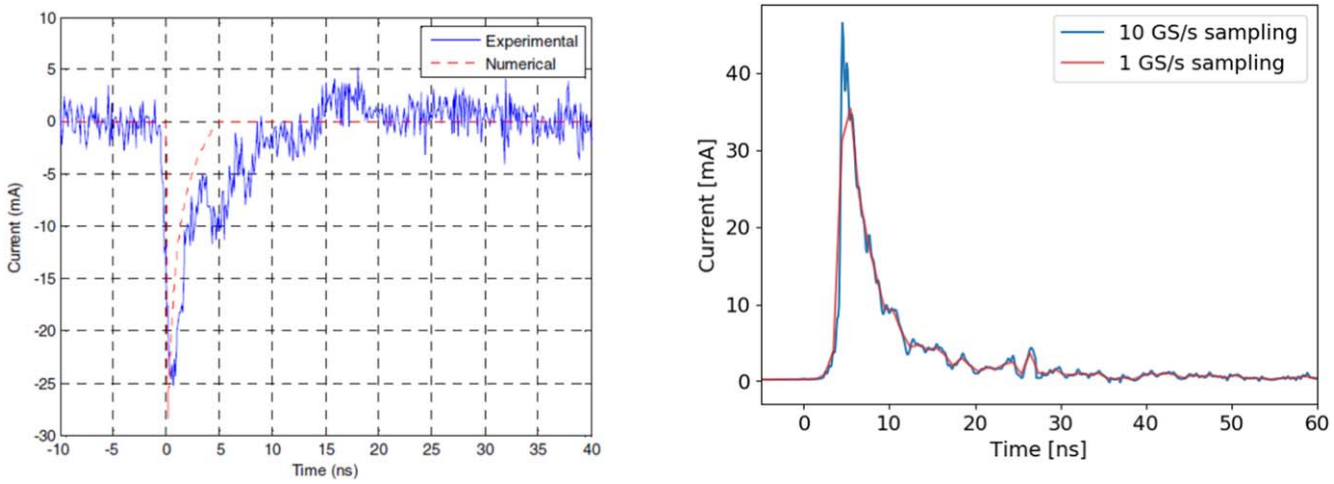

a) b)

Figure A2. Typical current waveforms corresponding to the streamer arrival to a dielectric-coated cathode in ambient air DBDs in a 50 μm wide dielectric cavity (a) (after Smith *et al* [302]) and in a single-filament volume barrier discharge with an air gap of 1mm (after Synek *et al* [55]).

ORCID iDs

Mirko Černák https://orcid.org/0000-0003-0939-5013
Tomáš Hoder https://orcid.org/0000-0001-5346-6275
Zdeněk Bonaventura https://orcid.org/0000-0002-9591-6040

References

[1] Siemens E W 1857 Poggendorff's *Ann. Phys. Chem.* **102** 66–122
[2] Rogowski W 1928 *Arch. Elektrotech.* **20** 99–106
[3] Raether H 1939 *Z.Phys.* **112** 464–89
[4] Loeb L B and Meek J M 1940 *J. Appl. Phys.* **11** 438–47
[5] Bruggeman P J, Iza F and Brandenburg R 2017 *Plasma Sources Sci. Technol.* **26** 123002
[6] Georghiou G E, Papadakis A P, Morrow R and Metaxas A C 2005 *J. Phys. D: Appl. Phys.* **38** R303
[7] Qin J and Pasko V P 2014 *J. Phys. D: Appl. Phys.* **47** 435202
[8] Brandenburg R 2017 *Plasma Sources Sci. Technol.* **26** 053001
[9] Becker K, Kogelschatz U, Schoenbach K and Barker R 2004 *Non-Equilibrium Air Plasmas at Atmospheric Pressure* (Boca Raton, FL: CRC Press)
[10] Mesyats G A 2007 *Pulsed Power* (New York: Springer Science & Business Media)
[11] Roth J 1995 *Industrial Plasma Engineering: vol 1: Principles Industrial Plasma Engineering* (Boca Raton, FL: CRC Press)
[12] Hogg M, Timoshkin I, MacGregor S, Wilson M and Given M 2015 *IEEE Trans. Dielectr. Electr. Insul.* **22** 1815–22
[13] Pedersen A 1989 *IEEE Trans. Electr. Insul.* **24** 721–39
[14] Hudson G G and Loeb L B 1961 *Phys. Rev.* **123** 29–43
[15] Eduard M and Bazelyan Y P R 1997 *Spark Discharge* (Boca Raton, FL: CRC Press)
[16] Paschen F 1889 *Ann. Phys.* **273** 69–96
[17] Townsend J 1910 *The Theory of Ionization of Gases by Collision* (London: Constable Ltd.)
[18] Franck J and Hertz G 1914 *Verh. Dtsch. Phys. Ges.* **16** 457–67
[19] Holst G *et al* 1923 *Phil. Mag.* **46** 1117
[20] Hodges R V, Varney R N and Riley J F 1985 *Phys. Rev.* A **31** 2610–20
[21] Rogowski W 1926 *Arch. Elektrotech.* **16** 496–508
[22] Schumann W 1923 *Elektrische Durchbruchfeldstaerke von Gasen* (Berlin: Springer)
[23] Meek J 1940 *Phys. Rev.* **57** 722
[24] Flegler E 1935 *Z. Tech. Phys.* **16** 435
[25] Loeb L B 1939 *Fundamental Processes of Electrical Discharge in Gases* (New York: Wiley)
[26] Amin M 1954 *J. Appl. Phys.* **25** 358–63
[27] Anderson N 1958 *Ark. Fys.* **13** 399–422
[28] Marode E 1975 *J. Appl. Phys.* **46** 2005–15
[29] Williams P F and Peterkin F E 1989 *J. Appl. Phys.* **66** 4163–75
[30] Ono R and Oda T 2003 *J. Phys. D: Appl. Phys.* **36** 1952
[31] Takahashi E, Kato S, Furutani H, Sasaki A, Kishimoto Y, Takada K, Matsumura S and Sasaki H 2011 *J. Phys. D: Appl. Phys.* **44** 302001
[32] Briels T, Kos J, Winands G, Van Veldhuizen E and Ebert U 2008 *J. Phys. D: Appl. Phys.* **41** 234004
[33] El-Zein A, Talaat M and Samir A 2018 *Vacuum* **156** 469–74
[34] Šimek M, Ambrico P F and Prukner V 2011 *Plasma Sources Sci. Technol.* **20** 025010
[35] Nudnova M M and Starikovskii A Y 2008 *J. Phys. D: Appl. Phys.* **41** 234003
[36] Luque A and Ebert U 2014 *New J. Phys.* **16** 013039
[37] Luque A, Ratushnaya V and Ebert U 2008 *J. Phys. D: Appl. Phys.* **41** 234005
[38] Pancheshnyi S, Nudnova M and Starikovskii A 2005 *Phys. Rev.* E **71** 016407
[39] Naidis G V 2009 *Phys. Rev.* E **79** 057401
[40] Shcherbakov Y and Sigmond R 2006 Novel high-resolved experimental results by sub-nanosecond spectral diagnostics of streamer discharges *37th AIAA Plasmadynamics and Lasers Conf.* p 3758
[41] Šimek M 2014 *J. Phys. D: Appl. Phys.* **47** 463001
[42] Dilecce G 2014 *Plasma Sources Sci. Technol.* **23** 015011
[43] Kondo K and Ikuta N 1980 *J. Phys. D: Appl. Phys.* **13** L33
[44] Kozlov K 2000 *7th Int. Symp. on High Pressure Low Temperature Plasma Chem. (HAKONE VII)* vol 1, pp 292–8
[45] Kozlov K V, Wagner H E, Brandenburg R and Michel P 2001 *J. Phys. D: Appl. Phys.* **34** 3164

[46] Shcherbakov Y V and Sigmond R 2007 *J. Phys. D: Appl. Phys.* **40** 460
[47] Hoder T, Černák M, Paillol J, Loffhagen D and Brandenburg R 2012 *Phys. Rev.* E **86** 055401
[48] Kozlov K V and Wagner H E 2007 *Contrib. Plasma Phys.* **47** 26–33
[49] Hoder T, Šimek M, Bonaventura Z, Prukner V and Gordillo-Vázquez F J 2016 *Plasma Sources Sci. Technol.* **25** 045021
[50] Naidis G V, Tarasenko V F, Babaeva N Y and Lomaev M I 2018 *Plasma Sources Sci. Technol.* **27** 013001
[51] Gravendeel B, van der Laan P and de Hoog F 1988 *J. Phys. D: Appl. Phys.* **21** 437
[52] Kondo K and Ikuta N 1990 *J. Phys. Soc. Japan* **59** 3203–16
[53] Wetzer J and Van Der Laan P 1989 *IEEE Trans. Electr. Insul.* **24** 297–308
[54] Eliasson B, Hirth M and Kogelschatz U 1987 *J. Phys. D: Appl. Phys.* **20** 1421
[55] Synek P, Zemanek M, Kudrle V and Hoder T 2018 *Plasma Sources Sci. Technol.* **27** 045008
[56] Odrobina I and Černák M 1995 *J. Appl. Phys.* **78** 3635–42
[57] Davies A, Davies C and Evans C 1971 *Proc. Inst. Electr. Eng.* **118** 816–23
[58] Kline L E and Siambis J G 1972 *Phys. Rev.* A **5** 794–805
[59] Kunhardt E E and Tzeng Y 1988 *Phys. Rev.* A **38** 1410–21
[60] Loeb L B 1948 *Rev. Mod. Phys.* **20** 151–60
[61] Morrow R and Lowke J 1997 *J. Phys. D: Appl. Phys.* **30** 614
[62] Chanrion O and Neubert T 2008 *J. Comput. Phys.* **227** 7222–45
[63] Won J Y and Williams P 2002 *J. Phys. D: Appl. Phys.* **35** 205
[64] Kulikovsky A 1998 *Phys. Rev.* E **57** 7066
[65] Pancheshnyi S 2005 *Plasma Sources Sci. Technol.* **14** 645
[66] Nijdam S, van de Wetering F M J H, Blanc R, van Veldhuizen E M and Ebert U 2010 *J. Phys. D: Appl. Phys.* **43** 145204
[67] Wormeester G, Pancheshnyi S, Luque A, Nijdam S and Ebert U 2010 *J. Phys. D: Appl. Phys.* **43** 505201
[68] Stephens J, Fierro A, Beeson S, Laity G, Trienekens D, P Joshi R, Dickens J and Neuber A 2016 *Plasma Sources Sci. Technol.* **25** 025024
[69] Kulikovsky A A 1998 *IEEE Trans. Plasma Sci.* **26** 1339–46
[70] Boeuf J P, Yang L L and Pitchford L C 2013 *J. Phys. D: Appl. Phys.* **46** 015201
[71] Nemschokmichal S *et al* 2018 *Eur. Phys. J.* D **72** 89
[72] Zhang Y, Gu B, Wang W, Wang D and Peng X 2009 *Spectrochim. Acta* A **72** 460–4
[73] Celestin S, Bonaventura Z, Zeghondy B, Bourdon A and Segur P 2009 *J. Phys. D: Appl. Phys.* **42** 065203
[74] Loeb L B 1965 *Science* **148** 1417–26
[75] Karakas E, Akman M A and Laroussi M 2012 *Plasma Sources Sci. Technol.* **21** 034016
[76] Boeuf J, Yang L and Pitchford L 2012 *J. Phys. D: Appl. Phys.* **46** 015201
[77] Stanley M, Krehbiel P, Brook M, Moore C, Rison W and Abrahams B 1999 *Geophys. Res. Lett.* **26** 3201–4
[78] Ebert U and Sentman D D 2008 *J. Phys. D: Appl. Phys.* **41** 230301
[79] Kunhardt E E 1980 *IEEE Trans. Plasma Sci.* **8** 130–8
[80] Warne K L, Jorgenson R E and Kunhardt E E 2014 *J. Appl. Phys.* **115** 143303
[81] Dhali S and Williams P 1987 *J. Appl. Phys.* **62** 4696–707
[82] McAllister I W, Crichton G C and Bregnsbo E 1979 *J. Appl. Phys.* **50** 6797–805
[83] Černák M, Kaneda T and Hosokawa T 1989 *Japan. J. Appl. Phys.* **28** 1989–96
[84] Laan M and Paris P 1994 *J. Phys. D: Appl. Phys.* **27** 970
[85] Brandenburg R, Kozlov K, Massines F, Michel P and Wagner H 2000 *Proceedings of 7th International Symposium on High Pressure Low Temperature Plasma Chemistry (HAKONE VII),* 1 *(Greifswald, Germany)* 93
[86] Chen Y, Zheng Y and Miao X 2017 *J. Appl. Phys.* **122** 033304
[87] Gallimberti I 1979 *J. Phys. Colloq.* **40** C7–193
[88] Kochkin P O, van Deursen A P and Ebert U 2014 *J. Phys. D: Appl. Phys.* **47** 145203
[89] Kunhardt E 1985 Pulsed breakdown in uniform electric fields *17th Int. Conf. on Phenomena in Ionized Gases (Budapest, Hungary)* pp 345–60
[90] Babaeva N Y, Zhang C, Qiu J, Hou X, Tarasenko V F and Shao T 2017 *Plasma Sources Sci. Technol.* **26** 085008
[91] Beloplotov D V, Lomaev M I, Sorokin D A and Tarasenko V F 2017 *Russ. Phys. J.* **60** 1308–13
[92] Marode E, Dessante P and Tardiveau P 2016 *Plasma Sources Sci. Technol.* **25** 064004
[93] Shao T, Zhang C, Niu Z, Yan P, Tarasenko V F, Baksht E K, Burahenko A G and Shutko Y V 2011 *Appl. Phys. Lett.* **98** 021503
[94] Babich L P and Stankevich Y L 1973 *Sov. Phys. Tech. Phys.* **17** 1333–6
[95] Lo A, Cessou A, Lacour C, Lecordier B, Boubert P, Xu D A, Laux C O and Vervisch P 2017 *Plasma Sources Sci. Technol.* **26** 045012
[96] Marode E 1981 *Nato ASI Ser.* B **89b** 119–66
[97] Doran A 1968 *Z. Phys.* **208** 427–40
[98] Koppitz J 1971 *Z. Nat.forsch.* **26** 700
[99] Chalmers I D, Duffy H and Tedford D 1972 *Proc. R. Soc.* A **239** 171
[100] Kremnev V V and Mesyats G A 1971 *J. Appl. Mech. Tech. Phys.* **12** 33–7
[101] Raether H 1964 *Electron Avalanches and Breakdown in Gases* (London: Butterworths)
[102] Montijn C and Ebert U 2006 *J. Phys. D: Appl. Phys.* **39** 2979
[103] Rabie M and Franck C M 2016 *J. Phys. D: Appl. Phys.* **49** 175202
[104] Llewellyn-Jones F 1983 The development of theories of the electrical breakdown of gases *Electrical Breakdown and Discharges in Gases: Fundamental Processes and Breakdown NATO ASI Series: Physics* ed E Kunhardt and L Luessen (Berlin: Springer) pp 1–71
[105] Fridman A, Chirokov A and Gutsol A 2005 *J. Phys. D: Appl. Phys.* **38** R1
[106] Cavenor M 1970 *Aust. J. Phys.* **23** 953–6
[107] Loeb L B 1951 *Phys. Rev.* **81** 287
[108] Davies A, Evans C and Woodison P 1975 *Proc. Inst. Electr. Eng.* **122** 765–8
[109] Davies A 1986 *IEE Proc.* A **133** 217–40
[110] Liu L and Becerra M 2017 *IEEE Trans. Plasma Sci.* **45** 594–602
[111] Palmer A J 1974 *Appl. Phys. Lett.* **25** 138–40
[112] Khomich V Y and Yamschikov V 2011 *Plasma Phys. Rep.* **37** 1182–9
[113] Babich L 2003 *High-Energy Phenomena in Electric Discharges in Dense Gases: Theory, Experiment and Natural Phenomena* (Arlington, VA: FuturepastCop. 2003)
[114] Casper L C, Bastiaens H M J, Peters P J M, Boller K J and Hofstra R M 2007 *Plasma Sources Sci. Technol.* **17** 015009
[115] Smy P and Clements R 1981 *J. Appl. Phys.* **52** 6576–83
[116] Belasri A, Boeuf J and Pitchford L 1993 *J. Appl. Phys.* **74** 1553–67
[117] Černák M, Bessieres D and Paillol J 2011 *J. Appl. Phys.* **110** 053303
[118] Makarov M 1995 *J. Phys. D: Appl. Phys.* **28** 1083
[119] Makarov M and Bychkov Y 1996 *J. Phys. D: Appl. Phys.* **29** 350
[120] Dreiskemper R, Schroder G and Botticher W 1995 *IEEE Trans. Plasma Sci.* **23** 180–7

[121] Mesyats G, Bychkov Y I and Isoldsky A 1968 *Zh. Tekh. Fiz* **38** 1281
[122] Mesyats G, Bychkov Y I and AI I 1969 *Sov. Phys. Tech. Phys.-USSR* **13** 1051
[123] Baksht E, Burachenko A, Kostyrya I, Lomaev M, Rybka D, Shulepov M and Tarasenko V 2009 *J. Phys. D: Appl. Phys.* **42** 185201
[124] Oshige T 1967 *J. Appl. Phys.* **38** 2528–34
[125] Naidis G 2005 *J. Phys. D: Appl. Phys.* **38** 3889
[126] Goldman M, Goldman A and Sigmond R 1985 *Pure Appl. Chem.* **57** 1353–62
[127] Kogelschatz U and Salge J 2008 *Low Temp. Plasmas* **2** 439
[128] Plewa J M, Eichwald O, Ducasse O, Dessante P, Jacobs C, Renon N and Yousfi M 2018 *J. Phys. D: Appl. Phys.* **51** 095206
[129] Kudu K, Lågstad I H and Sigmond R S 1998 *Czech. J. Phys.* **48** 1180–92
[130] Liu L and Becerra M 2016 *J. Phys. D: Appl. Phys.* **49** 225202
[131] Liu L and Becerra M 2017 *J. Phys. D: Appl. Phys.* **50** 105204
[132] Gosho Y and Saeki M 1987 *J. Phys. D: Appl. Phys.* **20** 526
[133] Teunissen J, Sun A and Ebert U 2014 *J. Phys. D: Appl. Phys.* **47** 365203
[134] Tarasenko V, Baksht E K, Sosnin E, Burachenko A, Panarin V and Skakun V 2018 *Plasma Phys. Rep.* **44** 520–32
[135] Nijdam S, van Veldhuizen E, Bruggeman P and Ebert U 2012 *Plasma Chemistry and Catalysis in Gases and Liquids: An Introduction to Nonequilibrium Plasmas at Atmospheric Pressure* (Weinheim: Wiley) pp 1–44
[136] Lowke J and D'Alessandro F 2003 *J. Phys. D: Appl. Phys.* **36** 2673
[137] El-Zein A E, Talaat M and Samir A 2017 *Am. J. Mod. Energy* **3** 95
[138] Cai Q, Jánský J and Pasko V P 2017 *Geophys. Res. Lett.* **44** 5758–65
[139] Qin J and Pasko V P 2014 *J. Phys. D: Appl. Phys.* **47** 435202
[140] Bessieres D, Paillol J, Gibert A and Pécastaing L 2005 *Plasma Process. Polym.* **2** 183–7
[141] Inada Y, Aono K, Ono R, Kumada A, Hidaka K and Maeyama M 2017 *J. Phys. D: Appl. Phys.* **50** 174005
[142] Sigmond R 1984 *J. Appl. Phys.* **56** 1355–70
[143] Loeb L B 1965 *Electrical Coronas, Their Basic Physical Mechanisms* vol 36 (Berkeley, CA: University of California Press)
[144] Hayakawa N, Ishiguro J, Kojima H, Kato K and Okubo H 2016 *IEEE Trans. Dielectr. Electr. Insul.* **23** 547–54
[145] Suzuki T 1971 *J. Appl. Phys.* **42** 3766–77
[146] Dawson G 1965 *J. Appl. Phys.* **36** 3391–5
[147] Inoshima M, Černák M and Hosokawa T 1990 *Japan. J. Appl. Phys.* **29** 1165
[148] Starikovskiy A, Nikipelov A and Rakitin A 2011 *IEEE Trans. Plasma Sci.* **39** 2606–7
[149] Larsson A 1998 *J. Phys. D: Appl. Phys.* **31** 1100
[150] Černák M, Van Veldhuizen E, Morva I and Rutgers W 1995 *J. Phys. D: Appl. Phys.* **28** 1126
[151] Merbahi N, Eichwald O, Dubois D, Abahazem A and Yousfi M 2007 Positive point-to-plane corona discharge in air: electrical and optical analysis *28th Int. Conf. on Phenomena in Ionized Gases (Prague, Czech Republic)* pp 963–6
[152] Eichwald O, Ducasse O, Dubois D, Abahazem A, Merbahi N, Benhenni M and Yousfi M 2008 *J. Phys. D: Appl. Phys.* **41** 234002
[153] Akishev Y, Karal'nik V and Trushkin N 2002 *Proc. SPIE* **4460** 26–37
[154] Peterkin F E and Williams P 1988 *Appl. Phys. Lett.* **53** 182–4
[155] Johnson P, Berger G and Goldman M 1977 *J. Phys. D: Appl. Phys.* **10** 2245
[156] Nasser E 1966 *J. Appl. Phys.* **37** 4712–6
[157] Uteza O, Delaporte P, Fontaine B, Forestier B, Sentis M and Tassy I 1998 *Appl. Phys.* B **67** 185–91
[158] Černák M, Hosokawa T and Inoshima M 1990 *Appl. Phys. Lett.* **57** 339–40
[159] Marode E, Bastien F and Bakker M 1979 *J. Appl. Phys.* **50** 140–6
[160] Komuro A and Ono R 2014 *J. Phys. D: Appl. Phys.* **47** 155202
[161] Ducasse O, Papageorghiou L, Eichwald O, Spyrou N and Yousfi M 2007 *IEEE Trans. Plasma Sci.* **35** 1287–300
[162] Komuro A and Ando A 2017 *Plasma Sources Sci. Technol.* **26** 065003
[163] Ducasse O, Eichwald O, Merbahi N, Dubois D and Yousfi M 2007 Numerical simulation and comparison with experiment for a positive point to plane corona discharges in dry air *28th Int. Conf. on Phenomena in Ionized Gases (Prague, Czech Republic)* pp 1046–49
[164] Beloplotov D V, Lomaev M I, Tarasenko V F and Sorokin D A 2018 *JETP Lett.* **107** 606–11
[165] Suzuki T 1975 *IEEE Trans. Power Appar. Syst.* **94** 1381–9
[166] Reess T, Ortega P, Gibert A, Domens P and Pignolet P 1995 *J. Phys. D: Appl. Phys.* **28** 2306
[167] Fark J H and Cones H N 1956 *J. Res. Natl Bur. Stand.* **56** 201–24
[168] Akazaki M and Tsuneyasu I 1977 Breakdown process of a rod to plane air gap under negative impulse voltage *13th Int. Conf. Phenomena in Ionized Gases* p 399
[169] Černák M and Hosokawa T 1988 *Appl. Phys. Lett.* **52** 185–7
[170] Isa H, Sonoi Y and Hayashi M 1991 *IEEE Trans. Electr. Insul.* **26** 291–9
[171] Zentner R 1970 *Z. Angew. Phys.* **29** 294
[172] Zentner R 1970 *ETZ-A* **91** 303–5
[173] Chanrion O and Neubert T 2008 *J. Comput. Phys.* **227** 7222–45
[174] Hagelaar G J M and Pitchford L C 2005 *Plasma Sources Sci. Technol.* **14** 722
[175] Scharfetter D L and Gummel H K 1969 *IEEE Trans. Electron Devices* **16** 64–77
[176] Hagelaar G 2008 *Habilitation à Diriger des Recherches* (France: Université de Toulouse)
[177] Hagstrum H D 1954 *Phys. Rev.* **96** 336–65
[178] Odrobina I and Černák M 1992 *Czech. J. Phys.* **42** 303–15
[179] Georghiou G, Morrow R and Metaxas A 2001 *J. Phys. D: Appl. Phys.* **34** 200
[180] Jánský J, Tholin F, Bonaventura Z and Bourdon A 2010 *J. Phys. D: Appl. Phys.* **43** 395201
[181] Poggie J, Adamovich I, Bisek N and Nishihara M 2013 *Plasma Sources Sci. Technol.* **22** 015001
[182] Becker M M, Kählert H, Sun A, Bonitz M and Loffhagen D 2017 *Plasma Sources Sci. Technol.* **26** 044001
[183] Li C, Ebert U and Hundsdorfer W 2010 *J. Comput. Phys.* **229** 200–20
[184] Kushner M J 2004 *J. Appl. Phys.* **95** 846–59
[185] Wang J C, Zhang D, Leoni N, Birecki H, Gila O and Kushner M J 2014 *J. Appl. Phys.* **116** 043301
[186] Chanrion O, Bonaventura Z, Çinar D, Bourdon A and Neubert T 2014 *Environ. Res. Lett.* **9** 055003
[187] Markosyan A H, Teunissen J, Dujko S and Ebert U 2015 *Plasma Sources Sci. Technol.* **24** 065002
[188] Soloviev V and Krivtsov V 2009 *J. Phys. D: Appl. Phys.* **42** 125208
[189] Aleksandrov N and Kochetov I 1996 *J. Phys. D: Appl. Phys.* **29** 1476
[190] Naidis G V 1997 *Tech. Phys. Lett.* **23** 493–4
[191] Babaeva N Y and Naidis G 2016 *Phys. Plasmas* **23** 083527
[192] Phelps A V and Pitchford L C 1985 *Phys. Rev.* A **31** 2932–49
[193] Kunhardt E, Tzeng Y and Boeuf J 1986 *Phys. Rev.* A **34** 440
[194] Davies A, Jones F and Evans C 1964 *Proc. R. Soc. Lond.* A **281** 164–83

[195] Davies A, Davies C and Evans C 1971 *Proc. Inst. Electr. Eng.* **118** 816
[196] Abbas I and Bayle P 1980 *J. Phys. D: Appl. Phys.* **13** 1055–68
[197] Morrow R 1985 *Phys. Rev.* A **32** 1799–809
[198] Duarte M, Bonaventura Z, Massot M, Bourdon A, Descombes S and Dumont T 2012 *J. Comput. Phys.* **231** 1002–19
[199] Chanrion O, Bonaventura Z, Cinar D, Bourdon A and Neubert T 2014 *Environ. Res. Lett.* **9** 055003
[200] LXcat, Biagi database www.lxcat.net, (Retrieved on 9 May, 2018)
[201] Biagi S 2005 Magboltz: Transport of electrons in gas mixtures CERN Program Library http://magboltz.web.cern.ch/magboltz/
[202] Černák M and Hosokawa T 1988 *Japan. J. Appl. Phys.* **27** 1005
[203] Josepson R 2004 Negative corona in N_2+O_2 mixtures *PhD Thesis, MSc Thesis* University of Tartu
[204] Černák M and Hosokawa T 1987 *Japan. J. Appl. Phys.* **26** L1721
[205] Černák M and Hosokawa T 1988 *Japan. J. Appl. Phys.* **27** 155
[206] Sigmond R 1978 *Electrical Breakdown of Gases* (Oxford: Oxford At The Clarendon Press) pp 319–85
[207] Lama W L and Gallo C F 1974 *J. Appl. Phys.* **45** 103–13
[208] Golinski J and Grudzinski J 1986 *J. Phys. D: Appl. Phys.* **19** 1497
[209] Laan M, Paris P and Repaen V 1997 *J. Phys. IV Colloq.* **7** 259–70
[210] Hoder T, Loffhagen D, Voráč J, Becker M and Brandenburg R 2016 *Plasma Sources Sci. Technol.* **25** 025017
[211] Trichel G W 1938 *Phys. Rev.* **54** 1078–84
[212] Loeb L B, Kip A F, Hudson G G and Bennett W H 1941 *Phys. Rev.* **60** 714–22
[213] Zentner R 1969 Der räumlich-zeitliche Aufbau der negativen impulsförmigen Koronaentladung *PhD Thesis* Universität Fridericiana Karlsruhe
[214] Goldman M and Goldman A 1978 *Gaseous Electronics* **1** 219–90
[215] Sigmond R and Torsethaugen K 1973 *11th Int. Conf. on Phenomena in Ionized Gases (Prague, Czech Republic)* p 194
[216] Gravendeel B and van der Laan P 1985 Fast current measurements in corona and laser-triggered corona-like discharges *8th Int. Conf. Gas Discharges and their Applications* pp 216–8
[217] Gravendeel B 1987 *Negative Corona Discharges: A Fundamental Study* (Eindhoven: Technische Universiteit Eindhoven)
[218] Kulkarni S and Nema R 1987 Broad band pulse detection studies of corona and breakdown in air, n 2, o 2, co 2, sf 6 and sf 6-n 2 mixtures *5th Int. Symp. on Gaseous Dielectrics* (Amsterdam: Elsevier) pp 637–42
[219] Graff D 1980 *Proc. 6th Int. Conf. on Gas Discharges, Edinburgh* pp 142–5
[220] Černák M, Hosokawa T, Kobayashi S and Kaneda T 1998 *J. Appl. Phys.* **83** 5678–90
[221] Tran T, Golosnoy I, Lewin P and Georghiou G 2010 *J. Phys. D: Appl. Phys.* **44** 015203
[222] Thanh L 1979 *Proc. Inst. Electr. Eng.* **126** 270–5
[223] Dordizadeh P, Adamiak K and Castle G P 2017 *J. Electrostat.* **88** 49–54
[224] Zhang Y, Qin Y, Zhao G and Ouyang J 2016 *J. Phys. D: Appl. Phys.* **49** 245206
[225] Laan M and Perelygin V 1991 The dependence of negative corona on electrode surface properties *20th Int Conf. on Phenomena in Ionized Gases* vol 4, pp 929–30
[226] Zahoranova A, Kudelcik J, Paillol J and Černák M 2002 *J. Phys. D: Appl. Phys.* **35** 762
[227] Meek J M and Craggs J D 1953 *Electrical Breakdown of Gases* (Oxford: Clarendon Press)
[228] Ikuta N and Kondo K 1976 A spectroscopic study of positive and negative coronas in nx/o, mixture'in'gas discharges' *IEE Conf. Publ* vol 143, pp 227–30
[229] Korge H and Laan M 1983 *16th Int. Conf. on Phenomena in Ionized Gases* pp 168–9
[230] Černák M and Hosokawa T 1991 *Phys. Rev.* A **43** 1107
[231] Černák M and Hosokawa T 1992 *Aust. J. Phys.* **45** 193–220
[232] Černák M, Hosokawa T and Odrobina I 1993 *J. Phys. D: Appl. Phys.* **26** 607
[233] Hoder T, Bonaventura Z, Bourdon A and Šimek M 2015 *J. Appl. Phys.* **117** 073302
[234] Ikuta N and Kondo K 1976 *Proc. 4th Int. Conf. on Gas Discharges* 227–39
[235] Hoder T, Hoeft H, Kettlitz M, Weltmann K D and Brandenburg R 2012 *Phys. Plasmas* **19** 070701
[236] Gupta D K, Mahajan S and John P 2000 *J. Phys. D: Appl. Phys.* **33** 681
[237] Bessieres D, Paillol J and Soulem N 2004 *J. Appl. Phys.* **95** 3943–51
[238] Napartovich A, Akishev Y S, Deryugin A, Kochetov I, Pan'kin M and Trushkin N 1997 *J. Phys. D: Appl. Phys.* **30** 2726
[239] Akishev Y S, Kochetov I, Loboiko A and Napartovich A 2002 *Plasma Phys. Rep.* **28** 1049–59
[240] Scott D and Haddad G 1986 *J. Phys. D: Appl. Phys.* **19** 1507
[241] Zheng Y, Wang L, Wang D and Jia S 2017 *Phys. Plasmas* **24** 063515
[242] Adamiak K and Malevanets A 2017 *J. Electrostat.* **87** 110–22
[243] Chen S, Li K and Nijdam S 2019 *Plasma Sources Sci. Technol.* **28** 055017
[244] Zheng Y, Wang L, Wang D and Jia S 2017 *Phys. Plasmas* **24** 063515
[245] Zhang Y, Qin Y, Zhao G and Ouyang J 2016 *J. Phys. D: Appl. Phys.* **49** 245206
[246] Chen S, Nobelen J and Nijdam S 2017 *Plasma Sources Sci. Technol.* **26** 095005
[247] Zhang Y, Xia Q, Jiang Z and Ouyang J 2017 *Sci. Rep.* **7** 10135
[248] Dordizadeh P, Adamiak K and Castle G P 2016 *J. Electrostat.* **84** 73–80
[249] Porteiro J, Martín R, Granada E and Patiño D 2016 *Fuel Process. Technol.* **143** 86–99
[250] Wang H Q, Jiang H L and Chen Y 2016 *Proc. Eng.* **135** 56–60
[251] Dhima P and Vila F 2018 *Adv. Mater. Phys. Chem.* **8** 387
[252] Aliat A, Tsai C J, Hung C T and Wu J S 2008 *Appl. Phys. Lett.* **93** 154103
[253] Villot A, Gonthier Y, Gonze E and Bernis A 2013 *J. Electrostat.* **71** 815–22
[254] Shi J J and Kong M G 2005 *Appl. Phys. Lett.* **86** 091502
[255] Kunhardt E E 2000 *IEEE Trans. Plasma Sci.* **28** 189–200
[256] Bruggeman P and Brandenburg R 2013 *J. Phys. D: Appl. Phys.* **46** 464001
[257] Akishev Y, Karalnik V, Kochetov I, Napartovich A and Trushkin N 2014 *Plasma Sources Sci. Technol.* **23** 054013
[258] Loeb L B 1949 *Phys. Rev.* **76** 255–9
[259] Bityurin V, Kulikovski A and Lyubimov G 1989 *Zh. Tekh. Fiz.* **59** 50–63
[260] Bityurin V and Kulikovski A 1989 *Proc. 19th Int. Conf. on Phenomena in Ionized Gases* ed M J Labat pp 106–7
[261] Zahoranová A, Černák M, Štefečka M and Wagner H E 1999 *Czech. J. Phys.* **49** 1721–35
[262] Cookson A H 1970 *Proc. Inst. Electr. Eng.* **117** 269–80
[263] Seeger M, Votteler T, Ekeberg J, Pancheshnyi S and Sanchez L 2018 *IEEE Trans. Dielectr. Electr. Insul.* **25** 2147–56

[264] Fu Y, Zhang P, Verboncoeur J P, Christlieb A J and Wang X 2018 *Phys. Plasmas* **25** 013530
[265] Akishev Y S, Grushin M E, Karal'nik V B and Trushkin N I 2001 *Plasma Phys. Rep.* **27** 520–31
[266] Mizeraczyk J, Berendt A and Akishev Y 2018 *J. Phys. D: Appl. Phys.* **51** 155204
[267] Korolev Y D, Frants O B, Landl N V, Bolotov A V and Nekhoroshev V O 2014 *Plasma Sources Sci. Technol.* **23** 054016
[268] Korolev Y D, Frants O B, Nekhoroshev V O, Suslov A I, Kas'yanov V S, Shemyakin I A and Bolotov A V 2016 *Plasma Phys. Rep.* **42** 592–600
[269] Waters R T 2019 *J. Phys. D: Appl. Phys.* **52** 025203
[270] Morávek T, Cech J, Navrátil Z and Ráhel' J 2016 *Eur. Phys. J. Appl. Phys.* **75** 24706
[271] Gherardi N and Massines F 2001 *IEEE Trans. Plasma Sci.* **29** 536–44
[272] Aleksandrov N L, Bazelyan E M, Gorunov A Y and Kochetov I V 1999 *J. Phys. D: Appl. Phys.* **32** 2636
[273] Akishev Y, Arefi-Khonsari F, Demir A, Grushin M, Karalnik V, Petryakov A and Trushkin N 2015 *Plasma Sources Sci. Technol.* **24** 065021
[274] Lowke J J and D'Alessandro F 2003 *J. Phys. D: Appl. Phys.* **36** 2673
[275] Alaya M, Chazelas C, Mariaux G and Vardelle A 2015 *J. Therm. Spray Technol.* **24** 3–10
[276] Aleksandrov N L and Bazelyan E M 2001 *Plasma Phys. Rep.* **27** 1057–78
[277] Allen K R and Phillips K 1963 *Proc. R. Soc.* A **274** 163–86
[278] Loeb L 1967 Pulsed breakdown in uniform electric fields *8th Int. Conf. on Phenomena in Ionized Gases (Vienna, Austria)* pp 345–60
[279] Arcese E, Rogier F and Boeuf J P 2017 *Phys. Plasmas* **24** 113517
[280] Park J, Henins I, Herrmann H W and Selwyn G S 2001 *J. Appl. Phys.* **89** 15–9
[281] Rusterholtz D L, Lacoste D A, Stancu G D, Pai D Z and Laux C O 2013 *J. Phys. D: Appl. Phys.* **46** 464010
[282] Stepanyan S, Minesi N, Tibère-Inglesse A, Salmon A, Stancu G D and Laux C O 2019 *J. Phys. D: Appl. Phys.* **52** 295203
[283] Obrusnik A, Bilek P, Hoder T, Simek M and Bonaventura Z 2018 *Plasma Sources Sci. Technol.* **27** 085013
[284] Bilek P, Obrusnik A, Hoder T, Simek M and Bonaventura Z 2018 *Plasma Sources Sci. Technol.* **27** 085012
[285] Dogariu A, Goldberg B M, O'Byrne S and Miles R B 2017 *Phys. Rev. Appl.* **7** 024024
[286] Patnaik A K, Adamovich I, Gord J R and Roy S 2017 *Plasma Sources Sci. Technol.* **26** 103001
[287] Loveless A M and Garner A L 2016 *Appl. Phys. Lett.* **108** 234103
[288] Teunissen J and Ebert U 2016 *Plasma Sources Sci. Technol.* **25** 044005
[289] Donko Z *et al* 2018 *Plasma Phys. Control. Fusion* **60** 014010
[290] Levko D and Raja L L 2018 *Phys. Plasmas* **25** 013509
[291] Bonitz M, Filinov A, Abraham J W and Loffhagen D 2018 *Plasma Sources Sci. Technol.* **27** 064005
[292] Bagheri B *et al* 2018 *Plasma Sources Sci. Technol.* **27** 095002
[293] Gibalov V I and Pietsch G J 2000 *J. Phys. D: Appl. Phys.* **33** 2618
[294] Hoder T, Brandenburg R, Basner R, Weltmann K D, Kozlov K V and Wagner H E 2010 *J. Phys. D: Appl. Phys.* **43** 124009
[295] Kogelschatz U 2002 *IEEE Trans. Plasma Sci.* **30** 1400–8
[296] Gibalov V, Samoilovich V and Filippov Y V 1981 *Russ. J. Phys. Chem.* **55** 471–9
[297] Braun D *et al* 1991 *J. Phys. D: Appl. Phys.* **24** 564
[298] Steinle G, Neundorf D, Hiller W and Pietralla M 1999 *J. Phys. D: Appl. Phys.* **32** 1350
[299] Ráhel' J, Šíra M, St'ahel P and Trunec D 2007 *Contrib. Plasma Phys.* **47** 34–9
[300] Yoshida K and Tagashira H 1986 *Mem. Kitami Inst. Technol.* **18** 11–20
[301] Yurgelenas Y V and Wagner H 2006 *J. Phys. D: Appl. Phys.* **39** 4031
[302] Smith D J, McMeekin S G, Stewart B G and Wallace P A 2012 The numerical modelling and experimental validation of a partial discharge within an air-filled cavity bound in oil impregnated paper *2012 IEEE Int. Symp. on Electrical Insulation* pp 117–21
[303] Hoeft H, Kettlitz M, Weltmann K D and Brandenburg R 2014 *J. Phys. D: Appl. Phys.* **47** 455202
[304] Höft H, Becker M M, Loffhagen D and Kettlitz M 2016 *Plasma Sources Sci. Technol.* **25** 064002
[305] Höft H, Becker M M and Kettlitz M 2016 *Phys. Plasmas* **23** 033504
[306] Höft H, Becker M M and Kettlitz M 2018 *Plasma Sources Sci. Technol.* **27** 03LT01
[307] Bartnikas R and Novak J P 1993 *IEEE Trans. Electr. Insul.* **28** 956–68
[308] Devins J C 1984 *IEEE Trans. Electr. Insul.* **EI-19** 475–95
[309] Morshuis P H F and Kreuger F H 1990 *J. Phys. D: Appl. Phys.* **23** 1562
[310] Starikovskaia S M 2006 *J. Phys. D: Appl. Phys.* **39** R265–99
[311] Gibalov V I and Pietsch G J 2012 *Plasma Sources Sci. Technol.* **21** 024010
[312] Benard N and Moreau E 2014 *Exp. Fluids* **55** 1846
[313] Leonov S B, Adamovich I V and Soloviev V R 2016 *Plasma Sources Sci. Technol.* **25** 063001
[314] Grosch H, Hoder T, Weltmann K D and Brandenburg R 2010 *Eur. Phys. J.* D **60** 547–53